

1 **Parameterization of biogeochemical sediment-water fluxes using**  
2 **in-situ measurements and a diagenetic model**

3 **Arnaud Laurent<sup>1\*</sup>, Katja Fennel<sup>1</sup>, Robin Wilson<sup>1</sup>, John Lehrter<sup>2</sup> and Richard Devereux<sup>2</sup>**

4 <sup>1</sup> Department of Oceanography, Dalhousie University, Halifax, Nova Scotia, Canada

5 <sup>2</sup> US EPA, Gulf Ecology Division, Gulf Breeze, USA

6 \* Corresponding author

7 E-mail: arnaud.laurent@dal.ca

8 **Abstract**

9 Diagenetic processes are important drivers of water column biogeochemistry in coastal areas.  
10 For example, sediment oxygen consumption can be a significant contributor to oxygen depletion  
11 in hypoxic systems, and sediment-water nutrient fluxes support primary productivity in the  
12 overlying water column. Moreover, non-linearities develop between bottom water conditions and  
13 sediment-water fluxes due to loss of oxygen-dependent processes in the sediment as oxygen  
14 becomes depleted in bottom waters. Yet, sediment-water fluxes of chemical species are often  
15 parameterized crudely in coupled physical-biogeochemical models, using simple linear  
16 parameterizations that are only poorly constrained by observations. Diagenetic models that  
17 represent sediment biogeochemistry are available, but rarely are coupled to water column  
18 biogeochemical models because they are computationally expensive. Here, we apply a method  
19 that efficiently parameterizes sediment-water fluxes of oxygen, nitrate and ammonium by  
20 combining *in situ* measurements, a diagenetic model and a parameter optimization method. As a

21 proof of concept, we apply this method to the Louisiana Shelf where high primary production,  
22 stimulated by excessive nutrient loads from the Mississippi-Atchafalaya River system, promotes  
23 the development of hypoxic bottom waters in summer. The parameterized sediment-water fluxes  
24 represent non-linear feedbacks between water column and sediment processes at low bottom  
25 water oxygen concentrations, which may persist for long periods (weeks to months) in hypoxic  
26 systems such as the Louisiana Shelf. This method can be applied to other systems and is  
27 particularly relevant for shallow coastal and estuarine waters where the interaction between  
28 sediment and water column is strong and hypoxia is prone to occur due to land-based nutrient  
29 loads.

## 30 **1. Introduction**

31 Sediment biogeochemistry represents a major component of elemental cycling on continental  
32 margins (Middelburg & Soetaert, 2005; Liu et al., 2010). In these shallow, productive areas on  
33 average 30% of photosynthetically produced organic matter is deposited and recycled in the  
34 sediment (Wollast, 1998). The recycling of this organic material consumes oxygen ( $O_2$ ) and can  
35 result in either a source or a sink of nutrients to the water column (Cowan and Boynton, 1996).  
36 For instance, a proportion of the deposited organic matter is remineralized via denitrification  
37 which produces biologically unavailable  $N_2$  gas. Denitrification represents a major removal  
38 pathway for nitrogen (N) in coastal areas (Fennel et al., 2009, Bohlen et al., 2012) and buffers  
39 the effects of excessive N loads in eutrophic systems (Seitzinger & Nixon, 1985). In this type of  
40 environment, high respiration rates in the water column and in the sediment may lead to bottom  
41  $O_2$  depletion under stratified conditions, resulting in bottom water hypoxia ( $O_2 < 62.5 \text{ mmol } O_2$   
42  $\text{m}^{-3}$ ) or anoxia (absence of  $O_2$ ). Under low  $O_2$  conditions, coupled nitrification-denitrification in  
43 the sediment is inhibited and remineralized N may return entirely to the water column as

44 ammonium ( $\text{NH}_4^+$ ), readily available to primary producers, which constitutes a positive feedback  
45 on eutrophication (Kemp et al., 1990). Conversely, N removal into  $\text{N}_2$  may increase due to direct  
46 denitrification or due to anammox if a source of nitrate/nitrite is available (Neubacher et al.,  
47 2012).  $\text{O}_2$ -dependent sediment-water interactions are therefore particularly important in low  $\text{O}_2$   
48 environments.

49       Clearly, the strong benthic-pelagic interaction is a key aspect of coastal biogeochemistry  
50 that needs to be represented accurately in biogeochemical models. However, sediment-water  
51 fluxes in models are often difficult to parameterize, being poorly constrained by observations.  
52 One of the simplest approaches to parameterizing sediment-water fluxes is using a reflective  
53 boundary where fluxes are proportional to particulate organic matter (POM) deposition (e.g.  
54 Fennel et al., 2006). Empirical relationships can be used to represent sediment biogeochemical  
55 processes, such as denitrification (Fennel et al., 2009) or sediment  $\text{O}_2$  consumption (SOC)  
56 (Hetland and DiMarco, 2008). An advantage of these first-order sediment-water flux  
57 parameterizations is that they are computationally extremely efficient and can be sufficient  
58 depending on the type of environment and the focus of the study (Wilson et al., 2013). However,  
59 sediment-water flux parameterizations are a coarse representation of sediment-water interaction  
60 and typically do not capture non-linearities in nutrient fluxes which occur under hypoxic/anoxic  
61 conditions. Moreover, the choice of parameterization can have a significant effect on model  
62 results as shown in Fennel et al. (2013) where different parameterizations of SOC led to  
63 dramatically different regions of hypoxia.

64       Mechanistic models of diagenesis are more realistic representations of sediment  
65 biogeochemistry (Rabouille & Gaillard, 1991; Soetaert & Herman, 1995; Soetaert et al., 1996a;  
66 DiToro, 2001, Meysman et al., 2003a,b). They are forced by POM deposition and bottom water

67 conditions, and simulate aerobic and anaerobic remineralization pathways including processes  
 68 such as nitrification, denitrification, the anaerobic production of reduced substances—  
 69 represented either explicitly or lumped together in O<sub>2</sub> demand units (ODU)—and the resulting  
 70 flux of O<sub>2</sub> and nutrients across the sediment-water interface. While these models have been  
 71 useful for studies of sediment biogeochemistry (Middelburg et al., 1996; Soetaert et al., 1996b;  
 72 Boudreau et al, 1998; Meysman et al., 2003b) and for improving our understanding of sediment-  
 73 water interactions (Katsev et al, 2007; Reed et al, 2011), their coupling to water column  
 74 processes in biogeochemical circulation models is often limited or done at the expense of spatial  
 75 resolution (Eldridge and Roelke, 2010) because of the increased computational cost.  
 76 Furthermore, the diagenetic model parameter sets are often poorly constrained by observations  
 77 and therefore these models do not necessarily perform better than the simple parameterizations  
 78 (Wilson et al., 2013).

79 An alternative, computationally more efficient approach is to parameterize sediment-  
 80 water fluxes from a diagenetic model using a meta-model of diagenetic processes, as  
 81 recommended by Soetaert et al. (2000). Their mass conservative method is more realistic than  
 82 the simple reflective boundary and computationally more efficient than a mechanistic model of  
 83 diagenesis. The method requires addition of a vertically integrated pool of sedimentary  
 84 particulate organic matter for each horizontal grid cell thus enabling a mass balanced approach,  
 85 but adding a layer of complexity to the water column model. Here we further simplify the meta-  
 86 modeling method of Soetaert et al (2000) by direct meta-modeling of sediment-water fluxes. Our  
 87 method parameterizes sediment-water fluxes of O<sub>2</sub>, NO<sub>3</sub><sup>-</sup> and NH<sub>4</sub><sup>+</sup> in a coupled biogeochemical  
 88 circulation model using in-situ measurements, a mechanistic model of early diagenesis and a  
 89 parameter optimization technique. The method is universal but its application is region-specific

90 due to the local characteristics of the sediment, e.g. sediment quality (POM concentration and  
91 lability), type (porosity) and species composition (bioturbation) that influence local sediment  
92 biogeochemistry and sediment-water fluxes and are reflected in the choice of diagenetic model  
93 parameters. We apply this method to the Louisiana Shelf in the northern Gulf of Mexico, where  
94 hypoxia develops annually due to eutrophication (Rabalais et al., 2002).

95 First, we calibrate the diagenetic model with the help of a genetic optimization algorithm  
96 using a set of observations collected on the Louisiana Shelf. We then implement the calibrated  
97 model to simulate time-resolved sediment biogeochemistry in the region and use the model  
98 results to compute a meta-model parameterization of sediment-water fluxes for  $O_2$ ,  $NH_4^+$  and  
99  $NO_3^-$ . Finally, we compare the fluxes parameterized with the meta-model with previous  
100 relationships used for the Louisiana Shelf.

## 101 **2. Materials and methods**

### 102 **2.1. Observations**

103 The data used for optimization of the diagenetic model parameters were collected at two  
104 locations along the 20 m isobath on the Louisiana Shelf (Figure 1) during 3 cruises in April, June  
105 and September 2006 (Murrell et al., 2013). The two locations experience hypoxia in summer but  
106 have distinct hydrographic and biological regimes. Station Z02 (see Murrell et al., 2013, for  
107 details on sampling design) is located off Terrebonne Bay on the eastern Louisiana Shelf and is  
108 influenced by river discharges from the Mississippi Delta with high primary productivity and  
109 high POM depositional flux. Station Z03 is located southwest of Atchafalaya Bay on the western  
110 Louisiana Shelf with somewhat higher salinity and lower chlorophyll concentrations than station  
111 Z02 (Lehrter et al., 2009; 2012). The dataset includes bottom water properties (temperature,

112 salinity, O<sub>2</sub> and nutrients, Table 1), sediment-water fluxes (O<sub>2</sub>, nutrients) and NH<sub>4</sub><sup>+</sup> sediment  
113 profiles (Figure 2). On each date, eight sediment cores were collected at each station (3 for O<sub>2</sub>  
114 flux, 3 for nutrient fluxes and 2 for sediment profiles). O<sub>2</sub> and nutrient fluxes were measured on  
115 site from triplicate individual incubations in sediment chambers. Sediment NH<sub>4</sub><sup>+</sup> concentration  
116 was measured for each 2 cm bin in the duplicate sediment cores. Bottom water temperature and  
117 salinity were measured with a CTD, whereas O<sub>2</sub> and nutrient concentrations were measured in  
118 the water overlying the sediment cores. Details on the dataset are available in Lehrter et al.  
119 (2012), Murrell et al. (2013) and Devereux et al. (2015).

## 120 **2.2. Sediment flux parameterization**

121 The parameterization of sediment-water fluxes was derived using output from a diagenetic  
122 model. The diagenetic model was first optimized using the observational dataset described in the  
123 previous section. The optimized diagenetic model was then run multiple times to derive meta-  
124 model parameterizations.

### 125 **2.2.1. Diagenetic model**

126 The diagenetic model represents the dynamics of the key constituents of the sediment (solids and  
127 pore water) involved in early diagenesis, as formulated by Soetaert et al. (1996a,b). The model is  
128 vertically resolved, and represents the upper 10 cm of the sediment using 10 layers with  
129 increasing resolution toward the surface. The diagenetic model has 6 state variables: the solid  
130 volume of organic carbon (OC), which is split into a labile class (which remineralizes rapidly)  
131 and a refractory class (which remineralizes slowly), NH<sub>4</sub><sup>+</sup>, NO<sub>3</sub><sup>-</sup>, O<sub>2</sub> and ODU. Reduced  
132 substances produced by anoxic remineralization are added to the ODU pool rather than being  
133 explicitly modeled. Model processes include aerobic remineralization, nitrification,

134 denitrification, anaerobic remineralization and ODU oxidation. Dissimilatory nitrate reduction to  
 135 ammonium (DNRA) and anaerobic ammonium oxidation (anammox) are not explicitly  
 136 represented in the model. Vertical transport of solid and pore water constituents depend on  
 137 sedimentation of POM to the sediment, and on diffusion, bioturbation and permanent burial. The  
 138 burial of ODU refers to the deposition of ODUs as solids (e.g., pyrite, manganese carbonate)  
 139 below the bioturbated zone (Soetaert et al., 1996a). The model simulates sediment-water fluxes  
 140 of pore water constituents, namely  $\text{NH}_4^+$ ,  $\text{NO}_3^-$ ,  $\text{O}_2$  and ODU. We assume that ODUs are oxidized  
 141 instantaneously in the water column when  $\text{O}_2$  is available. Therefore, the net  $\text{O}_2$  flux into the  
 142 sediment is the addition of the direct  $\text{O}_2$  flux necessary for nitrification, oxidation of ODUs and  
 143 of POM in the sediment, termed SOC, plus the  $\text{O}_2$  sink in bottom waters necessary to oxidize any  
 144 ODU efflux from the sediment.

145 The original model of Soetaert et al. (1996a,b) was modified as follows. A temperature-  
 146 dependency was introduced for the remineralization of the two organic matter pools and the  
 147 bioturbation of solids following a  $Q_{10}$  relationship such that:

$$R_i(T) = R_i^{T_b} \times \theta^{(T-T_b)/10} \quad (1)$$

148 where  $R_i(T)$  and  $R_i^{T_b}$  ( $\text{y}^{-1}$ ) are the remineralization or bioturbation at ambient temperature ( $T$ ;  
 149  $^{\circ}\text{C}$ ) and at the base temperature ( $T_b$ ;  $^{\circ}\text{C}$ ) (i.e.,  $R_1^{T_b}$  and  $R_2^{T_b}$  for remineralization and  $\text{Dbio}_0$  for  
 150 bioturbation, Table 2) and  $\theta$  is the  $Q_{10}$  factor. In the updated model temperature thus influences  
 151 the solute diffusivity, the degradability of the two OM pools and bioturbation. This modification  
 152 allows for the representation of temperature-dependence of microbial processes in the sediment  
 153 (aerobic respiration, denitrification and anaerobic metabolism), which is known to be important

154 in coastal systems (see, e.g., Fig. 5 in Wilson et al. 2013). Nitrification is not temperature  
 155 dependent in the diagenetic model. It is assumed that O<sub>2</sub> concentration is the main factor limiting  
 156 nitrification in the Louisiana Shelf sediments.

157 Non-local mixing of pore water constituents due to bioturbation (irrigation) was also  
 158 introduced and formulated following Boudreau (1997) such that:

$$I(z) = \alpha(z) \cdot (C_{ow} - C(z)) \quad (2)$$

159 where  $I(z)$  ( $\mu\text{mol L}^{-1} \text{y}^{-1}$ ) is the irrigation at depth  $z$ ,  $C_{ow}$  and  $C(z)$  ( $\mu\text{mol L}^{-1}$ ) are the solute  
 160 concentration at the sediment-water interface and at depth  $z$  in the sediment, respectively.  $\alpha(z)$  is  
 161 the rate of non-local exchanges at depth  $z$  such that  $\alpha(z) = \alpha_0 \cdot f(z)$ , where  $\alpha_0$  ( $\text{y}^{-1}$ ) is the rate at  
 162  $z = 0$  and  $f(z)$  is a function representing the decay of  $\alpha$  with depth. Here,  $f(z)$  is the same  
 163 function as for the bioturbation of solids (Soetaert et al., 1996a). Bioturbation and non-local  
 164 mixing of solutes are not dependent on O<sub>2</sub> in the model. Such a dependence could be introduced  
 165 to account for repeated cycles of eradication/re-establishment of macrofauna due to anoxia.  
 166 However, given the limited information on the relationship between porewater O<sub>2</sub>, infauna  
 167 biomass and irrigation in this region (Eldridge and Morse, 2008), we assumed that macrobiota  
 168 does not re-establish itself in the regions affected by recurring severe seasonal hypoxia or anoxia  
 169 on the Louisiana Shelf and thus do not expect a strong dependence of bioturbation and  
 170 bioirrigation on O<sub>2</sub>.

171 The model has a total of 36 parameters (Table 2). Sediment porosity parameters were  
 172 chosen to obtain a porosity profile that is within the range observed on the Louisiana Shelf.  
 173 Given a lack of observations, the nitrogen to carbon ratio (N:C; mol N (mol C)<sup>-1</sup>) of the labile  
 174 and refractory fraction of OC were fixed to constant values following Wilson et al. (2013). The

175 assumption is that N:C follows Redfield (Redfield et al., 1963) in the labile fraction (N:C =  
 176 0.15), whereas the proportion of carbon increases in the refractory fraction (N:C = 0.10). Since  
 177 deposited OC mainly originates from local primary production on the shallow Louisiana Shelf  
 178 (Redalje et al., 1994; Justić et al., 1996; Rowe and Chapman, 2002), labile OC is assumed to  
 179 represent 74% of total OC in deposited material. This value was used by Soetaert et al. (1996a)  
 180 to represent the fraction of labile organic matter in surface waters and is in line with previous  
 181 modeling investigations of the Louisiana Shelf (Justić et al., 1996; Eldridge and Morse, 2008).  
 182 However, inshore areas adjacent to river discharge may have higher fraction of terrestrial organic  
 183 matter. The exponential decay coefficient for bioturbation was set as in the original model  
 184 (Soetaert et al., 1996a).

185 Solute-specific diffusion coefficients ( $D_i^T$ ;  $\text{cm}^2 \text{d}^{-1}$ ) at ambient temperature  $T$  were  
 186 calculated following Soetaert et al. (1996a) and Li & Gregory (1974) such that  $D_i^T = D_i + \alpha_i T$ ,  
 187 where  $D_i$  ( $\text{cm}^2 \text{d}^{-1}$ ) is the solute-specific diffusion coefficient at  $0^\circ\text{C}$  and  $\alpha_i$  ( $\text{cm}^2 \text{d}^{-1} (\text{°C})^{-1}$ ) is the  
 188 solute-specific temperature dependency coefficient (Table 2). The 20 remaining parameters of  
 189 the diagenetic model (Table 2) were optimized to obtain the best match between the observed  
 190 and simulated sediment profiles and sediment-water fluxes.

191 **2.2.2. Parameter optimization**

192 The diagenetic model parameters were first optimized to match the sediment-water fluxes  
 193 and sediment  $\text{NH}_4^+$  concentrations observed in April, June and September 2006 at station Z02  
 194 and Z03. The sampling frequency at these stations did not allow construction of a reasonable  
 195 time-dependent forcing dataset for the diagenetic model (i.e. solute concentrations in overlying  
 196 water, POM deposition). Thus, we didn't run the optimization in a time-dependent mode; instead

197 the model was run for 300 days with constant forcing for each time and location where  
198 observations were available. During the optimization the model was forced with observed  
199 bottom water conditions, namely salinity, temperature,  $\text{NH}_4^+$ ,  $\text{NO}_3^-$ , and  $\text{O}_2$  (Table 1). Since no  
200 observations of POM depositional flux were available, POM depositional fluxes were prescribed  
201 using monthly means calculated for station Z02 and Z03 from a multiyear biogeochemical model  
202 simulation (see Section 2.2.3). The mean depositional fluxes do not represent short-lived  
203 deposition events which is appropriate for a model with constant forcing.

204 Optimization of the parameter set was carried out with the help of an evolutionary  
205 algorithm. This stochastic technique mimics natural selection by iteratively selecting the “fittest”  
206 set of parameters to reproduce the observations. The evolutionary algorithm is a well accepted  
207 method for optimization problems (Hibbert, 1993; Fogel, 1994; Chatterjee et al., 1996; Kolda et  
208 al., 2003) and has been increasingly used to optimize parameters in biogeochemical models  
209 (Kuhn et al., 2015; Robson et al., 2008; Schartau and Oschlies, 2003; Ward et al., 2010). The  
210 technique was successfully used for the optimization of parameters of Soetaert et al.’s (1996a)  
211 diagenetic model in two independent studies (Wilson et al., 2013; Wood et al., 2013). The  
212 advantage of the evolutionary algorithm over traditionally used gradient-descent algorithms is  
213 that it explores the parameter space with an element of randomness and therefore is less prone to  
214 converging on a local minimum. Each parameter is given a range of variation within which the  
215 algorithm will search for the best value to match the observations. Regardless of which  
216 minimization technique is used, gradient-descent or an evolutionary algorithm, some parameters  
217 may not be identifiable because they are unconstrained by the available observations (Soetaert et  
218 al., 1998; Fennel et al., 2001).

219           The evolutionary algorithm works as follows. Each set of parameters is considered to be  
220 a single individual. An initial set of  $n$  individuals includes the initial parameter set and  $n - 1$   
221 individuals generated randomly from this initial set of parameters through the addition of log-  
222 normally distributed random noise. The diagenetic model is run with the  $n$  parameter sets, and  
223 the difference between the results and observations is quantified using a cost function, which  
224 measures the misfit between the observations and their model counterparts. The fittest  $n/2$   
225 individuals, i.e. those with the lowest cost, become the parent population and a next generation  
226 of  $n/2$  individuals (child population) is created by recombination of the parameters from the  
227 fitter half of the population and by mutation, which occurs through the addition of random noise.  
228 The model is run again for all the parameter sets of the child population, and the above procedure  
229 repeated for  $k$  generations. The fittest individual after  $k$  generations is the optimized parameter  
230 set. Here, we used  $n = 30$  population members and  $k = 200$  generations. The chosen value of  $k$   
231 is large enough to allow the results to converge.

232           Ideally a single parameter set should capture the temporal and spatial variability of  
233 sediment processes throughout the Louisiana Shelf. For this reason, the diagenetic model was  
234 run with identical parameters in all 6 model configurations (3 dates, 2 locations), each  
235 corresponding to a set of observed bottom water conditions plus estimated  $F_{\text{POM}}$  (Table 1).  
236 Model results were compared with their corresponding set of sediment observations ( $\text{NH}_4^+$   
237 porewater concentrations and sediment-water fluxes) using a cost function that includes all  
238 model variables at the 6 locations/times. The smaller the cost, the fitter is an individual (i.e.  
239 parameter set) during the evolutionary optimization process. The cost function  $F$  for the  
240 parameter set  $\vec{p}$  was calculated as follows:

$$F(\mathbf{p}) = \sum_{s=1}^l \sum_{t=1}^m \left( \sum_{i=1}^n \left( \frac{1}{w_i} \times \frac{(X_{s,t,i}^{mod}(\vec{p}) - X_{s,t,i}^{obs})^2}{\sigma_{s,t,i}^2} \right) \right) \quad (3)$$

241 where  $s$  refers to locations Z02 and Z03,  $t$  is the sampling date (3 in 2006) and  $i$  is the  
 242 observation type: 3 sediment-water fluxes (SOC,  $\text{NH}_4^+$  and  $\text{NO}_3^-$ ) and 1 sediment profile ( $\text{NH}_4^+$ ).  
 243  $X^{obs}$  and  $X^{mod}$  represent the observed and simulated variable, respectively;  $\sigma_{s,t,i}^2$  is the  
 244 observation standard deviation; and  $1/w_i$  represents the weight of each variable in the cost  
 245 function. The values of  $w_i$  were calculated for each variable  $i$  as the cost of a diagenetic model  
 246 run using the initial parameter set  $\mathbf{p}_0$  such that  $w_i = F_i(\mathbf{p}_0)$ . The weight gives the variables  
 247 approximately equal influence on the overall cost, at least initially. The weighting approach is  
 248 common in parameter optimization studies (see, e.g., Friedrichs, 2001; Schartau and Oschlies,  
 249 2003; Friedrichs et al., 2007; Kane et al., 2011). To avoid biasing the cost calculation toward the  
 250  $\text{NH}_4^+$  profiles we computed an average cost per profile.

251 The sensitivity of the optimized model to parameter changes was assessed by  
 252 successively varying each parameter by  $\pm 50\%$  and calculating the change in the total cost. Then  
 253 the influence of observations and forcing datasets on the optimization results was assessed as  
 254 follows. First, the optimization was carried out for each station individually (to obtain site-  
 255 specific parameters); then sediment profiles were excluded from the optimization (to obtain site-  
 256 specific parameters optimized for flux data only) and, finally, POM depositional fluxes were  
 257 included as additional parameters in the optimization rather than prescribed (to obtain site-  
 258 specific parameters and  $F_{\text{POM}}$  optimized for flux data only).

### 259 **2.2.3. Meta-modeling procedure**

260 Our meta-modeling procedure parameterizes sediment-water fluxes by means of a multivariate  
261 regression model that relates bottom water conditions and depositional flux to sediment-water  
262 fluxes, and was used here to parameterize Louisiana Shelf fluxes at the sediment-water interface.  
263 Using a meta-model of sediment-water fluxes is a simplification of the method proposed by  
264 Soetaert et al. (2000) who used a meta-model of diagenetic processes (rates) instead. The aim of  
265 our technique is to combine the simplicity and efficiency of a sediment-water flux  
266 parameterization with the realism of a diagenetic model. It is important to note that our  
267 simplified meta-model is not mass conservative; however, as long as the method is used for the  
268 system for which it was developed and within the range of conditions that were used for the  
269 parameterization, violation of mass conservation should be minor. An advantage of our  
270 simplification is that it does not require knowledge of integrated POM concentration in the  
271 sediment.

272 In order to obtain the meta-model parameterization the diagenetic model was run many  
273 times in time-varying mode using the single parameter set optimized for the Louisiana Shelf. The  
274 diagenetic model was forced with multi-year time series of bottom water conditions obtained  
275 from a biogeochemical circulation model of the Louisiana Shelf based on the Regional Ocean  
276 Modeling System (ROMS; Figure 3). The simulation is described in Fennel et al. (2013) (case  
277 B20clim) and covers the period from 2004 to 2009. The same simulation was used to prescribe  
278 POM depositional fluxes during the parameter optimization. For details on the model set up and  
279 validation we refer the reader to Fennel et al. (2013). We included only those grid cells on the  
280 Louisiana Shelf ( $z < 50$  m) and west of the Mississippi River delta. Each grid cell (3791 in total)  
281 provides a time series of bottom water temperature, salinity,  $\text{NO}_3^-$ ,  $\text{NH}_4^+$ ,  $\text{O}_2$  and POM  
282 depositional flux conditions that was used to run the optimized diagenetic model. We consider

283 2004 as a spin up year for the diagenetic model and selected the period 2005-2009 for analysis.  
 284 Half of the data from each simulation were randomly chosen to derive the meta-model. The  
 285 multivariate meta-model regressions were then calculated to relate bottom water conditions and  
 286 depositional flux (model inputs) to the corresponding sediment-water fluxes (model output)  
 287 using the  $3.45 \cdot 10^6$  data vectors. To validate the meta-model we calculated correlation  
 288 coefficients between the remaining data of each diagenetic model simulation (i.e. at each model  
 289 grid location) and the corresponding meta-model results.

290 Each regression model is expressed as follows:

$$y = a + \sum_{i=1}^n (b_i x_i + c_i x_i^2 + d_i x_i^3) \quad (4)$$

291 where each  $x_i$  corresponds to an explanatory variable  $i$ , and  $a$ ,  $b_i$ ,  $c_i$  and  $d_i$  are the coefficients  
 292 for the zero-order term, the regular term ( $x_i$ ), the squared term ( $x_i^2$ ) and the cubic term ( $x_i^3$ ),  
 293 respectively.

### 294 **2.3. Other flux parameterizations**

295 The meta-model parameterizations are compared with three other sediment-water flux  
 296 parameterizations that have been used previously in our biogeochemical circulation model for  
 297 the northern Gulf of Mexico (reviewed by Fennel et al., 2013). All three parameterizations  
 298 represent SOC and  $\text{NH}_4^+$  flux only. The first (Eq. 5-6), referred to as IR, assumes instantaneous  
 299 remineralization of deposited PON into  $\text{NH}_4^+$  while a fraction of N is lost through denitrification.  
 300 IR is formulated as follows (Fennel et al., 2006; 2009):

$$F_{\text{NH}_4^+}^{\text{IR}} = r_{\text{NH}_4^+} \cdot (w_P \text{Phy} + w_S \text{SDet} + w_L \text{LDet}), \quad (5)$$

$$F_{\text{O}_2}^{\text{IR}} = -r_{\text{O}_2:\text{NH}_4^+} F_{\text{NH}_4^+}^{\text{IR}}, \quad (6)$$

301 with  $r_{\text{NH}_4^+} = 4/16$  mmol  $\text{NH}_4^+$  per mol PON and  $r_{\text{O}_2:\text{N}} = 115/16$  mmol  $\text{O}_2$  per mol  $\text{NH}_4^+$ .  $w_P$ ,  
 302  $w_S$  and  $w_L$  are the sinking rate of phytoplankton (Phy) and small (SDet) and large (LDet)  
 303 detritus, respectively.

304 The other two parameterizations assume that SOC depends on bottom water  $\text{O}_2$  and  
 305 temperature ( $T$ ) only and ignore POM deposition. One, referred to as H&D (Eq. 7), is from  
 306 Hetland & DiMarco (2008). The other, referred to as M&L (Eq. 8), is from Murrell & Lehrter  
 307 (2011) with a temperature-dependence added by Fennel et al. (2013). Sediment-water  $\text{O}_2$  fluxes  
 308 are formulated as follows:

$$F_{\text{O}_2}^{\text{H\&D}} = 6 \cdot 2^{T/10} \cdot (1 - e^{-\text{O}_2/30}), \quad (7)$$

$$F_{\text{O}_2}^{\text{M\&L}} = 0.0235 \cdot 2^{T/10} \cdot \text{O}_2, \quad (8)$$

309 For each parameterization  $x$  the sediment-water  $\text{NH}_4^+$  flux is a function of SOC such that:

$$F_{\text{NH}_4^+}^x = -r_{\text{NH}_4^+:\text{SOC}} F_{\text{O}_2}^x, \quad (9)$$

310 with  $r_{\text{NH}_4^+:\text{SOC}} = 0.036$  mmol  $\text{NH}_4^+$  per mmol  $\text{O}_2$ .

311 **3. Results**312 **3.1. Diagenetic model parameter optimization**

313 Optimization of the diagenetic model parameters lowered the cost function (Eq. 3) significantly  
314 compared to the original parameter set (Table 3).  $\text{NH}_4^+$  profiles and sediment-water fluxes  
315 simulated with the optimized parameters are, in most cases, within two standard deviations of the  
316 observations (Figure 2). Simulated  $\text{O}_2$  fluxes match the observations at station Z02 but are  
317 underestimated somewhat in April and June at station Z03. Observed  $\text{O}_2$  fluxes are relatively  
318 high in April and June at station Z03 despite low sediment-water nutrient fluxes and  $\text{NH}_4^+$   
319 concentration in the sediment. Observed  $\text{O}_2$  flux had a very large standard deviation in April at  
320 station Z03 and therefore did not influence the optimization.  $\text{NH}_4^+$  and  $\text{NO}_3^-$  fluxes represent a  
321 more difficult problem for the optimization and therefore their cost is larger, especially at station  
322 Z03. Overall, sediment-water fluxes are better simulated at station Z02 and therefore station Z03  
323 contributes more the total cost for the optimized parameter set (Table 3). Temporal variations in  
324  $\text{NH}_4^+$  and  $\text{NO}_3^-$  fluxes are in qualitative agreement with observations although the model  
325 underestimates their magnitudes (Figure 2). The model is able to simulate observed  $\text{NO}_3^-$  flux  
326 realistically, in particular the observed  $\text{NO}_3^-$  flux into the sediment under low bottom  $\text{O}_2$   
327 conditions (Figure 2). Within the sediment, simulated  $\text{NH}_4^+$  concentrations agree with  
328 observations in April and June, but are underestimated in September. High  $\text{NH}_4^+$  concentrations  
329 were observed at station Z02 at this time despite low  $\text{NH}_4^+$  effluxes from the sediment. Note that  
330 the observations have large standard deviations for this case and therefore this  $\text{NH}_4^+$  sediment  
331 profile had only a small influence on the optimization. Some of the observed  $\text{NH}_4^+$  profiles in  
332 April and September display a gradient at depth (Figure 2) that the diagenetic model might not

333 be able to resolve. There is also a deep negative gradient in the simulated profiles in April  
 334 indicating that the model didn't reach full steady state conditions at depth. However, this  
 335 mismatch at depth has a limited effect on sediment-water fluxes.

336         Within the optimized parameter set, several parameter values reached the lower or upper  
 337 edge of their allowed range, which can be informative about the dynamics of the system (Table  
 338 2). Except for the bioturbation diffusivity ( $D_{bio}$ ), all other parameters associated with  
 339 bioturbation reduced the effect of bioturbation on sediment-water fluxes over the course of the  
 340 optimization: the depth of the bioturbated layer ( $z_{bio}$ ) decreased to 1 cm; the optimized  $Q_{10}$  factor  
 341 for bioturbation ( $\theta_{bio}$ ) moved to the lower limit of the  $Q_{10}$  range ( $2 < \theta < 3$ ); and the non-local  
 342 mixing coefficient ( $\alpha_0$ ) was reduced to a small value essentially removing the influence of non-  
 343 local mixing from the system. In addition to the reduction in bioturbation, permanent burial of  
 344 ODUs does not occur in the optimized model ( $PB = 0$ , Table 2). Conversely, the optimized  $Q_{10}$   
 345 factors for the remineralization of the slow ( $\theta_{r1}$ ) and fast ( $\theta_{r2}$ ) decaying pools of organic matter  
 346 are at their upper limits indicating a strong dependence of remineralization on temperature  
 347 (Table 2). For denitrification, the optimized value for the inhibition effect of  $NO_3^-$  ( $k_{dnf}$ ) is low  
 348 compared to the original parameter, whereas the inhibition effect of  $O_2$  ( $k_{indnf}$ ) is high (Table 2).  
 349 The inhibition effect of  $O_2$  on nitrification ( $k_{nit}$ ) and of  $NO_3^-$  ( $k_{inanox}$ ) and  $O_2$  ( $k_{inodu}$ ) on anaerobic  
 350 remineralization is small in comparison to the original parameters. The maximum rate of  
 351 nitrification (Nit) is significantly higher than in the original parameter set (Table 2).

352         We examined the sources of model-data discrepancies by sequentially releasing part of  
 353 the constraints on the parameter optimization (Figure 2, Table 3). Optimizing station Z02 and  
 354 Z03 separately improves the total cost by decreasing the cost associated with  $NH_4^+$  and  $NO_3^-$

355 fluxes (Table 3), in particular for  $\text{NO}_3^-$  at station Z02 (Figure 3, Table 3). Removing the  
 356 constraint of sediment  $\text{NH}_4^+$  profiles from the optimization improves the total cost further  
 357 (Table 3). This is due, in part, to the absence of  $\text{NH}_4^+$  profiles from the cost calculation, but also  
 358 to somewhat improved sediment-water fluxes (Figure 2). The best agreement between simulated  
 359 and observed sediment-water fluxes is achieved by including POM depositional fluxes as  
 360 additional parameter to optimize (Figure 3, Table 3). In this case POM deposition is increased in  
 361 June ( $\times 2$  and  $\times 1.3$  at station Z02 and Z03, respectively) and reduced in spring ( $\times 0.5$  and  $\times 0.25$   
 362 at station Z02 and Z03, respectively) and fall ( $\times 0.5$  at station Z03) and the cost associated with  
 363  $\text{NO}_3^-$  and  $\text{NH}_4^+$  fluxes decreases significantly (Table 3). However, when  $\text{NH}_4^+$  profiles are not  
 364 included in the cost calculation there is a large deviation between observed and modeled  
 365 sediment  $\text{NH}_4^+$  concentrations (not included in the cost). The root mean square error for the  
 366 sediment profiles increases from  $87.59 \text{ mmol N m}^{-2} \text{ d}^{-1}$  for the baseline case to  $174.45 \text{ mmol N}$   
 367  $\text{m}^{-2} \text{ d}^{-1}$  (*Site-specific, flux only*) and  $111.86 \text{ mmol N m}^{-2} \text{ d}^{-1}$  (*Site-specific, flux only +  $F_{POM}$* ).  
 368 Since the parameter set with all constraints best represents sediment-water fluxes and  $\text{NH}_4^+$   
 369 sediment concentrations throughout the Louisiana Shelf, it is used subsequently to parameterize  
 370 sediment-water fluxes and is referred to as baseline.

371 For most of the parameter set, the optimized model is insensitive to parameter variation  
 372 (Figure 5). The most sensitive process in the diagenetic model is the remineralization of the fast  
 373 decaying organic matter pool, since the optimized model is sensitive to all the associated  
 374 parameters, namely the remineralization of the fast decaying organic matter pool ( $R_2(T)$ ), the  
 375 base temperature ( $T_b$ ) and the  $Q_{10}$  factor for fast decaying organic matter ( $\theta_{r1}$ ) in the  $Q_{10}$   
 376 relationship. The optimized model is also sensitive to the variation in POM deposition rates at

377 station Z03 ( $F_{\text{POM}3x}$ ), mainly in June. Variation in deposition rates at station Z02, however, does  
 378 not influence the overall cost. The sensitivity to parameters or model forcing related to organic  
 379 matter is not surprising given the high magnitude and large temporal and spatial variations in  
 380 POM deposition in this region. Nonetheless, it highlights the overall uncertainty in the optimized  
 381 model due to the lack of observations on depositional flux. The difference in sensitivities to the  
 382 depositional flux at stations Z02 and Z03 can be explained by the magnitude of the total cost,  
 383 which is higher at station Z03 (Table 3). The cost at station Z02 is sensitive to the POM  
 384 deposition rate (e.g. >300% increase in April), but since the cost at station Z03 is much higher,  
 385 the effect on the total cost is small. The uncertainty associated with POM deposition rates is then  
 386 larger at station Z03. To a lesser extent, the optimized model is sensitive to the bioturbation  
 387 diffusivity ( $D_{\text{bio}0}$ ) and to the maximum rate of nitrification (Nit). The cost is largest for  $\text{NO}_3^-$  flux  
 388 (Table 3), which indicates that the optimization has more difficulty fitting the observations for  
 389 this flux. The sensitivity of the optimized value for nitrification rate, which influence  $\text{NO}_3^-$  flux,  
 390 is therefore higher.

391 **3.2. Meta-modeling parameterization**

392 A meta-model of sediment-water fluxes was derived using simulations with the optimized  
 393 diagenetic model, as described in section 2.2.3. The coefficients of the meta-model  
 394 parameterizations for  $\text{O}_2$ ,  $\text{NH}_4^+$  and  $\text{NO}_3^-$  sediment-water fluxes and the range of bottom water  
 395 conditions used for the parameterization are presented in Table 4. Each parameterization is able  
 396 to reproduce the sediment-water fluxes simulated with the diagenetic model (Figure 6). The  
 397 spatially resolved correlation coefficients are above 0.8 for most of the Louisiana Shelf for  $\text{O}_2$   
 398 and  $\text{NH}_4^+$  fluxes and above 0.6 for  $\text{NO}_3^-$  fluxes (Figure 6). The parameterization fails to retrieve

399 the simulated fluxes in some limited areas near the offshore limit of the shelf. Bottom water  
 400 conditions for depths greater than 50 m were not included in the meta-modeling  
 401 parameterization, which explains why the meta-model does not perform well at a few limited  
 402 areas along the 50 m isobath.

403 Overall, the main contributors to the meta-model are temperature, salinity and O<sub>2</sub> (Table  
 404 4). The average contribution of POM deposition is low (Table 4, Figure 7). The time dependency  
 405 between POM deposition and sediment-water fluxes is implicit in the meta-model and therefore  
 406 instant POM deposition is not a good predictor of sediment-water fluxes. Temperature is the  
 407 largest contributor for all fluxes (Table 4) and is associated with the seasonal variation in  
 408 sediment-water fluxes. Salinity is not included in the diagenetic model but is a significant  
 409 contributor in the meta-model because it is associated with the spatial variation in sediment-  
 410 water fluxes on the Louisiana Shelf. Bottom water O<sub>2</sub> has a growing effect on NH<sub>4</sub><sup>+</sup> and NO<sub>3</sub><sup>-</sup> flux  
 411 under hypoxic conditions (Table 4, Figure 6). When bottom water O<sub>2</sub> is low, NH<sub>4</sub><sup>+</sup> flux increases  
 412 with decreasing O<sub>2</sub>. More deposited particulate organic N is thus returned to the water column as  
 413 NH<sub>4</sub><sup>+</sup>. O<sub>2</sub> concentration controls both the direction and intensity of NO<sub>3</sub><sup>-</sup> flux in the meta-model.  
 414 With oxygenated bottom waters, NO<sub>3</sub><sup>-</sup> flux depends on bottom NO<sub>3</sub><sup>-</sup> concentration due to NO<sub>3</sub><sup>-</sup>  
 415 diffusion across the sediment-water interface. NO<sub>3</sub><sup>-</sup> flux is into the sediment when the bottom  
 416 water NO<sub>3</sub><sup>-</sup> concentration is high and out of the sediment when the bottom water NO<sub>3</sub><sup>-</sup>  
 417 concentration is low. When bottom waters are hypoxic, NO<sub>3</sub><sup>-</sup> flux is oriented into the sediment,  
 418 which then becomes a sink for water column NO<sub>3</sub><sup>-</sup> (Figure 7).

419 By using simulated bottom water conditions from our biogeochemical circulation model  
420 as input for the meta-model we can assess the spatial and temporal variability in parameterized  
421 sediment-water fluxes over the Louisiana Shelf (see Figure 8 and 9). Sediment-water fluxes were  
422 computed from the meta-model in mid August 2009 (Figure 8) and throughout 2009 at station  
423 Z02 and Z03 (Figure 9). Bottom water conditions are presented in Figure 3. The spatial  
424 distribution of parameterized  $O_2$  and  $NH_4^+$  fluxes are somewhat similar (Figure 8), with large  
425 fluxes near Atchafalaya Bay and the Mississippi River delta where POM deposition is high in  
426 late Spring ( $> 5 \text{ mmol N m}^{-2} \text{ d}^{-1}$ , Figure 3). Patches of moderate to high  $NH_4^+$  flux ( $1\text{--}4 \text{ mmol N}$   
427  $\text{m}^{-2} \text{ d}^{-1}$ ) occur southwest of Terrebonne Bay and further west on the shelf where bottom waters  
428 are hypoxic (Figure 8).  $NO_3^-$  flux follows the distribution of bottom water  $O_2$  on the shelf with  
429 flux into the sediment in hypoxic areas and flux out of the sediment elsewhere (Figure 8).

430 The time series at stations Z02 and Z03 indicate high temporal variability in  
431 parameterized sediment-water fluxes in summer (Figure 9) that are driven by rapid changes in  
432 bottom water conditions (Figure 3). The difference in the magnitude of  $O_2$  flux is large between  
433 the two stations and coincides with the distinct POM deposition rate at the two stations in spring  
434 and early summer (Figure 9). This time-dependent effect is implicit in the meta-model. A similar  
435 pattern occurs for  $NH_4^+$  flux at station Z02 (Figure 9). The annual peak in  $NH_4^+$  flux occurs under  
436 hypoxic conditions. In late summer and fall, transient hypoxic conditions at station Z03 result in  
437 enhanced  $NH_4^+$  flux to the water column. The direction and magnitude of  $NO_3^-$  fluxes closely  
438 follows the  $O_2$  concentration in bottom water. Hypoxic conditions starting in early July at station  
439 Z02 result in a switch from efflux of  $NO_3^-$  from the sediment to influx of  $NO_3^-$  into the sediment

440 (Figure 9). As for  $\text{NH}_4^+$ , rapid reversal in  $\text{NO}_3^-$  flux direction in late summer and fall at station  
441 Z03 is associated with changes between oxic and hypoxic conditions.

### 442 **3.3. Comparison with other parameterizations**

443 Here we explore the differences between the meta-models and the three sediment-water flux  
444 parameterizations we used previously in our ROMS models for the Louisiana Shelf, i.e. IR,  
445 which assumes instant remineralization of deposited POM, and H&D and M&L, which are  
446 functions of bottom temperature and  $\text{O}_2$  concentration only. In contrast to the H&D and M&L  
447 parameterizations,  $\text{O}_2$  flux has a relatively weak sensitivity to bottom water  $\text{O}_2$  concentrations in  
448 the meta-model (Figure 10).  $\text{O}_2$  flux decreases at low bottom water  $\text{O}_2$  concentration but does not  
449 stop in anoxic conditions, as it is the case for H&D and M&L. In the model, at low  $\text{O}_2$ , ODUs  
450 become the dominant  $\text{O}_2$  sink (due to ODU oxidation in the water column) and therefore the  $\text{O}_2$   
451 sink can be significant despite the lack of  $\text{O}_2$  in bottom waters. Similar to the IR  
452 parameterization,  $\text{O}_2$  flux increases with PON depositional flux, but this effect is much weaker in  
453 the meta-model (Figure 10).

454 The  $\text{NH}_4^+$  flux parameterized with the meta-model falls within the range of the H&D and  
455 M&L parameterizations when  $\text{O}_2$  is available ( $\text{O}_2 > 50 \text{ mmol O}_2 \text{ m}^{-3}$ , Figure 11). However, the  
456 meta-model differs significantly from H&D and M&L in hypoxic conditions;  $\text{NH}_4^+$  flux increases  
457 with decreasing  $\text{O}_2$ , opposite to the H&D and M&L parameterizations. As for  $\text{O}_2$  flux, the  
458 increase in  $\text{NH}_4^+$  flux with PON deposition is weaker than in the IR parameterization (Figure 11).  
459 In the meta-model, the  $\text{NH}_4^+$  flux is larger than in IR under hypoxic conditions and low PON  
460 deposition, and lower than in IR at high deposition.

461 Sediment-water fluxes were calculated by applying the meta-models to output from the  
462 biogeochemical circulation model and are compared to those parameterized with the H&D  
463 parameterization (Figure 12). O<sub>2</sub> fluxes are larger in the meta-model in the areas of hypoxia near  
464 the Mississippi and Atchafalaya river mouths and on the mid shelf (see Figure 7). O<sub>2</sub> fluxes are  
465 smaller in the meta-model in other regions, especially on the western Louisiana Shelf where  
466 bottom water salinity and O<sub>2</sub> concentrations are elevated. NH<sub>4</sub><sup>+</sup> flux is also much higher in the  
467 meta-model in regions where hypoxia occurs (Figure 12). In the other areas NH<sub>4</sub><sup>+</sup> flux is slightly  
468 lower in the meta-model.

#### 469 **4. Discussion**

470 The meta-model procedure for parameterizing sediment-water fluxes requires a diagenetic model  
471 that realistically represents sediment processes. In order to obtain such a realistic diagenetic  
472 model for the Louisiana Shelf we optimized a modified version of Soetaert et al.'s model  
473 (1996a), which captures the main temporal variations in sediment biogeochemistry, sediment  
474 NH<sub>4</sub><sup>+</sup> concentration and sediment-water fluxes at the two sampling locations on the eastern and  
475 western Louisiana Shelf. An issue with the optimization of large parameter sets in diagenetic  
476 models is the poor identifiability of some parameters that results in a large uncertainty in their  
477 value (Soetaert et al., 1998). This caveat in our optimization approach would not be alleviated by  
478 using a different type of optimization. Several methods have been proposed to estimate  
479 parameter identifiability and uncertainty (Soetaert et al., 1998; Soetaert and Petzoldt, 2010,  
480 Fennel et al. 2001). However, a more complete set of observations would be necessary. The  
481 available observations were also not sufficient to allow running the diagenetic model in a time-  
482 dependent mode and therefore the optimization was carried out with constant forcing conditions.  
483 To evaluate the effect of parameter variations (i.e. uncertainty) on the model results we carried

484 out a sensitivity analysis on the optimized model. A key driver of diagenetic processes is POM  
485 deposition and the remineralization of the labile deposited POM is the most sensitive parameter  
486 in the model. Observations of POM deposition were not available and using average rates of  
487 POM deposition from a biogeochemical model, as we have done here, is an additional source of  
488 uncertainty. This is demonstrated by the improved agreement between simulated and observed  
489 sediment-water fluxes when including POM deposition in the optimization.

490         Some of the discrepancies between model and observations can also be attributed to the  
491 imposition of a single parameter set. For example, sediment porosity and bioturbation are  
492 interdependent (Mulsow et al., 1998) and influence sediment-water fluxes (Aller, 1982). They  
493 are known to vary spatially on the Louisiana Shelf (Lehrter et al., 2012; Briggs et al., 2014),  
494 which is not represented in the optimized parameter set. This limitation could be resolved by  
495 introducing spatially dependent bioturbation and porosity coefficients; however, a much larger  
496 spatially resolved dataset would be necessary to obtain these dependencies. Another limitation is  
497 the observed deep gradient in some of the  $\text{NH}_4^+$  profiles (e.g. in April), whereas the diagenetic  
498 model imposes a no gradient boundary condition a depth. Some mismatch between model and  
499 observations may also be generated by missing processes in the diagenetic model. As in earlier  
500 studies of the Louisiana Shelf (Morse and Eldridge, 2007; Eldridge and Morse, 2008), the  
501 diagenetic model does not represent DNRA and anammox. Although DNRA can be an important  
502 contributor to the N cycle under severe hypoxia (Dale et al., 2013), there is a poor understanding  
503 of the importance of DNRA on the Louisiana Shelf due to the lack of observations (Dagg et al.,  
504 2007). High porewater sulphide concentrations near the sediment-water interface are not reported  
505 for sediments of the Louisiana Shelf (Lin and Morse, 1991; Morse and Eldridge, 2007), which  
506 tend to minimize the importance of DNRA. However, the large  $\text{NH}_4^+$  porewater concentrations

507 observed at station Z02 in September (Figure 2) could be explained by the occurrence of DNRA.  
508 Anammox may also be a sink for bottom water  $\text{NH}_4^+$  on the Louisiana Shelf (Lin et al., 2011).  
509 McCarthy et al. (2015) found that anammox may represent, at times, up to 30% of denitrification  
510 (including anammox) in some locations of the Louisiana Shelf. As a result,  $\text{NH}_4^+$  flux to the  
511 water column may be overestimated by the diagenetic model, and in the parameterization, under  
512 low bottom  $\text{O}_2$  conditions.

513 Overall, despite some discrepancies with observations primarily due to uncertainty about  
514 POM deposition, diagenetic processes are represented reasonably well in the optimized model.  
515 Therefore, we deemed the optimized model as an appropriate framework for representing the  
516 main diagenetic processes on the Louisiana Shelf. Further development of the diagenetic model  
517 may include explicit anaerobic reactions, including DNRA and anammox. However, this is  
518 beyond the scope of this work.

519 Comparing optimized parameters to the original parameter set used by Soetaert et al.  
520 (1996a) is informative about sediment biogeochemistry on the Louisiana Shelf. The  
521 optimization minimized the influence of bioturbation, likely a reflection of the negative impact  
522 of hypoxia on sediment biota (Diaz & Rosenberg, 1995; Middelburg & Levin, 2009). This result  
523 is also consistent with the dominance of bacteria over invertebrates in the sediment community  
524 as observed by Rowe et al. (2002). The small  $\text{O}_2$  and  $\text{NO}_3^-$  inhibition parameters for anaerobic  
525 remineralization emphasize the importance of anaerobic processes in the area (Morse and  
526 Berner, 1995). This is consistent with observations for Mississippi River plume sediments that  
527 suggest a substantial production of reduced substances under low  $\text{O}_2$  conditions throughout the  
528 Louisiana Shelf (Rowe et al., 2002; Lehrter et al., 2012) and reflects the important role of ODU

529 in the  $O_2$  flux meta-model. The small optimized value for  $NO_3^-$  limitation of denitrification  
530 indicates that direct denitrification is an important process on the Louisiana Shelf when low  $O_2$   
531 limits coupled nitrification-denitrification (Nunnally et al., 2013). Direct denitrification occurs  
532 when  $NO_3^-$  is available in bottom waters and tends to increase with increasing  $NO_3^-$  concentration  
533 (Fennel et al., 2009). The small optimized value of  $O_2$  inhibition on nitrification and the  
534 relatively high maximum rate of nitrification compared to the original parameter values are also  
535 indications that sediment nitrification is an important process on the Louisiana Shelf,  
536 contributing to  $O_2$  consumption in the sediment. This result is also consistent with earlier  
537 observations (Lehrter et al., 2012).

538         We added temperature dependence of remineralization to the original model from  
539 Soetaert et al. (1996a). Model results were very sensitive to changes in the remineralization of  
540 the fast decaying organic matter pool ( $R_2(T)$ ). The optimum temperature of remineralization  
541 ( $T_{opt}$ ), the remineralization at optimum temperature ( $R_2^{T_{opt}}$ ) and the  $Q_{10}$  parameter for the fast  
542 decaying organic matter pool ( $\theta_2$ ) all influence  $R_2(T)$  and therefore model results are very  
543 sensitive to variations in these parameter values.

544         The meta-model reproduced the results from the optimized diagenetic model remarkably  
545 well suggesting that it is possible to use such parameterizations in place of a full, vertically  
546 resolved diagenetic model to prescribe sediment-water boundary conditions in biogeochemical  
547 circulation models. Previous meta-model parameterizations of diagenetic rates (Middelburg et  
548 al., 1996; Soetaert et al., 2000; Gypens et al., 2008) and perturbation response experiments  
549 (Rabouille et al., 2001) had similar success. The present method is somewhat different because  
550 the goal is to parameterize sediment-water exchanges directly as a function of bottom water

551 conditions. This simplified parameterization method does not require an additional, vertically-  
 552 integrated sediment layer to track deposited POM as in the method proposed by Soetaert et al.  
 553 (2000). Although the meta-model is not mass conservative, violation of mass conservation  
 554 should be minor if the meta-model is used for the system and within the range of conditions that  
 555 were used for its development. The resulting meta-model exhibits realistic dynamics such as the  
 556 increase of sediment-water fluxes in summer due to warmer temperature and the time delay  
 557 between POM deposition and remineralization, the decrease of coupled nitrification-  
 558 denitrification at low bottom O<sub>2</sub> concentrations and the prominent role of reduced substances  
 559 (represented by the ODU pool) as an O<sub>2</sub> sink in suboxic conditions.

560         Perhaps a key difference to other sediment-water parameterizations is the importance of  
 561 ODU at low O<sub>2</sub>, which results in a relatively weak relationship between O<sub>2</sub> flux and bottom O<sub>2</sub>  
 562 concentration in hypoxic conditions, and the occurrence of O<sub>2</sub> flux in anoxic conditions; in the  
 563 meta-model, ODU is the dominant source of O<sub>2</sub> consumption in hypoxic conditions and at high  
 564 temperature (i.e., in summer), independently of bottom O<sub>2</sub> concentration. Previous  
 565 parameterizations of sediment-water O<sub>2</sub> flux on the Louisiana Shelf considered only SOC and  
 566 therefore O<sub>2</sub> flux decreased toward zero with decreasing bottom O<sub>2</sub> in the hypoxic range (with a  
 567 zero intercept for anoxic conditions). However, Lehrter et al. (2012) found an increase of the  
 568 DIC/O<sub>2</sub> flux ratio with bottom O<sub>2</sub> depletion that they attributed to anaerobic metabolism, i.e. the  
 569 production of reduced chemical species that accumulate in the sediment, diffuse back and  
 570 reoxidize in the water column when O<sub>2</sub> becomes available. Justić and Wang (2014) considered  
 571 the effect of reduced chemical species on biological oxygen demand in their hypoxia model. It  
 572 represents a significant O<sub>2</sub> sink in bottom waters and needs to be accounted for in the sediment-  
 573 water O<sub>2</sub> flux parameterization. The O<sub>2</sub> flux meta-model combines SOC and ODU fluxes and is

574 therefore a more realistic representation of  $O_2$  consumption at the sediment-water interface. This  
 575 formulation assumes instant ODU oxidation in the water column, even in anoxic conditions,  
 576 whereas oxidation occurs in oxygenated waters only. The time delay between ODU flux and  
 577 oxidization is therefore missing in the meta-model but is accounted for if the coupled  
 578 biogeochemical-circulation model carries an  $O_2$  debt in anoxic conditions, as is the case in the  
 579 models of Fennel et al. (2009, 2013) and Laurent and Fennel (2014).

580         The meta-model simulates both the  $O_2$  dependence of coupled nitrification-denitrification  
 581 and direct denitrification, which are also key differences to simple parameterizations of  
 582 sediment-water fluxes in biogeochemical models. The inhibition of coupled nitrification-  
 583 denitrification at low  $O_2$  stimulates eutrophication and therefore represents a positive feedback of  
 584 hypoxia, as observed in Chesapeake Bay and other eutrophic systems (Kemp et al., 1990) and  
 585 estimated for the global coastal ocean (Rabouille et al., 2001). It is essential to represent this  
 586 feedback in high N/low  $O_2$  systems such as the Louisiana Shelf. In the  $NO_3^-$  meta-model, the  
 587 inhibition of coupled nitrification-denitrification in hypoxic conditions is partly compensated by  
 588 the increase in direct denitrification in areas where  $NO_3^-$  is available in bottom waters, which  
 589 results in a nitrate flux to the sediment. On the Louisiana Shelf, this is the case in areas near the  
 590 Mississippi-Atchafalaya River source, especially in the shallow area near Atchafalaya Bay. The  
 591 parameterized nitrate uptake by the sediment agrees with observations from the Louisiana Shelf  
 592 (Gardner et al., 1993; Nunnally et al., 2013). Nunnally et al. (2013) suggest a limited coupling  
 593 between nitrification and denitrification in the Louisiana Shelf hypoxic zone. Nonetheless, the  
 594 magnitude of this  $NO_3^-$  sink remains much smaller than the  $NH_4^+$  flux to the water column and

595 therefore the overall effect of low bottom O<sub>2</sub> is an enrichment of N in the water column, i.e. a  
596 positive feedback on eutrophication.

597 The meta-model method can be easily implemented in biogeochemical circulation  
598 models. However, the method should be applied only on regional scales because different types  
599 of bacterial, meio- or macrofaunal communities with various levels of bioturbation are associated  
600 with distinct types of substrate, porosity and POM quality and quantity affect POM recycling and  
601 thus influence the rates of sediment diagenetic processes locally (Herman et al., 1999). In other  
602 words, diagenetic models are region-specific.

## 603 **5. Summary and conclusions**

604 Benthic-pelagic coupling in biogeochemical circulation models is usually implemented through  
605 simple parameterizations or with a diagenetic model. These methods are either too simplistic or  
606 computationally very costly. Soetaert et al. (2000) proposed an intermediate method to improve  
607 the efficiency of benthic-pelagic coupling in biogeochemical circulation models. Here we  
608 presented a simplified version computing a meta-model of sediment-water fluxes for use in a  
609 regional biogeochemical model through optimization of a diagenetic model. The method results  
610 in a realistic and computationally efficient representation of sediment-water fluxes. Applied to  
611 the Louisiana Shelf, the method provides insight in the sediment biogeochemistry of the region,  
612 such as the importance of anaerobic processes and reduced substances, the limited level of  
613 bioturbation, the occurrence of direct denitrification and the inhibition of coupled nitrification-  
614 denitrification in hypoxic conditions. The meta-models represent these Louisiana shelf processes,  
615 resulting in more realistic, non-linear interactions between POM deposition, bottom water

616 concentrations and sediment-water fluxes, in particular under hypoxic conditions. A potential  
617 limitation of the method is the need for local observations to optimize the diagenetic model.

## 618 **Acknowledgements**

619 This work was supported by NOAA CSCOR grants NA06N0S4780198 and NA09N0S4780208  
620 and the US IOOS Coastal Ocean Modeling Testbed. NOAA NGOMEX publication no. XXX.

## 621 **References**

- 622 Aller, Robert, C.: The effects of macrobenthos on chemical properties of marine sediment and  
623 overlying water, in *Animal-sediment relations*, pp. 53–102., 1982.
- 624 Boudreau, B. P.: *Diagenetic models and their implementation: modelling transport and reactions*  
625 *in aquatic sediments*, Springer., 1997.
- 626 Boudreau, B. P., Mucci, A., Sundby, B., Luther, G. W. and Silverberg, N.: Comparative  
627 diagenesis at three sites on the Canadian continental margin, *J. Mar. Res.*, 56(6), 1259–1284,  
628 doi:10.1357/002224098765093634, 1998.
- 629 Briggs, K. B., Cartwright, G., Friedrichs, C. T. and Shivarudruppa, S.: Biogenic effects on  
630 cohesive sediment erodibility resulting from recurring seasonal hypoxia on the Louisiana shelf,  
631 *Cont. Shelf Res.*, 1–10, doi:10.1016/j.csr.2014.11.005, 2014.
- 632 Chatterjee, S., Laudato, M. and Lynch, L. A.: Genetic algorithms and their statistical  
633 applications: an introduction, *Comput. Stat. Data Anal.*, 22(6), 633–651, doi:10.1016/0167-  
634 9473(96)00011-4, 1996.
- 635 Cowan, J. L. W. and Boynton, W. R.: Sediment-Water Oxygen and Nutrient Exchanges along  
636 the Longitudinal Axis of Chesapeake Bay: Seasonal Patterns, Controlling Factors and Ecological  
637 Significance, *Estuaries*, 19(3), 562–580, doi:10.2307/1352518, 1996.
- 638 Dagg, M., Ammerman, J., Amon, R., Gardner, W., Green, R. and Lohrenz, S.: A review of water  
639 column processes influencing hypoxia in the northern Gulf of Mexico, *Estuaries Coasts*, 30(5),  
640 doi:10.1007/BF02841331, 735–752, 2007.
- 641 Dale, A. W., Bertics, V. J., Treude, T., Sommer, S. and Wallmann, K.: Modeling benthic–pelagic  
642 nutrient exchange processes and porewater distributions in a seasonally hypoxic sediment:  
643 evidence for massive phosphate release by *Beggiatoa?*, *Biogeosciences*, 10(2), 629–651,  
644 doi:10.5194/bg-10-629-2013, 2013.

- 645 Devereux, R., Lehrter, J. C., Beddick, D. L., Yates, D. F. and Jarvis, B. M.: Manganese, iron, and  
 646 sulfur cycling in Louisiana continental shelf sediments, *Cont. Shelf Res.*, 99, 46–56,  
 647 doi:10.1016/j.csr.2015.03.008, 2015.
- 648 Diaz, R. J. and Rosenberg, R.: Marine benthic hypoxia: a review of its ecological effects and the  
 649 behavioural responses of benthic macrofauna, *Oceanogr. Mar. Biol. an Annu. Rev.*, 33, 245–303,  
 650 1995.
- 651 DiToro, D. M.: *Sediment flux modeling*, Wiley and Sons, New York., 2001.
- 652 Eldridge, P. M. and Morse, J. W.: Origins and temporal scales of hypoxia on the Louisiana shelf:  
 653 Importance of benthic and sub-pycnocline water metabolism, *Mar. Chem.*, 108(3-4), 159–171,  
 654 doi:10.1016/j.marchem.2007.11.009, 2008.
- 655 Eldridge, P. M. and Roelke, D. L.: Origins and scales of hypoxia on the Louisiana shelf:  
 656 importance of seasonal plankton dynamics and river nutrients and discharge, *Ecol Model.*,  
 657 221(7), 1028–1042, doi:10.1016/j.ecolmodel.2009.04.054, 2010.
- 658 Fennel, K., Losch, M., Schröter, J. and Wenzel, M.: Testing a marine ecosystem model:  
 659 sensitivity analysis and parameter optimization, *J. Mar. Syst.*, 28(1-2), 45–63,  
 660 doi:10.1016/S0924-7963(00)00083-X, 2001.
- 661 Fennel, K., Wilkin, J., Levin, J., Moisan, J., O'Reilly, J. and Haidvogel, D.: Nitrogen cycling in  
 662 the Middle Atlantic Bight: Results from a three-dimensional model and implications for the  
 663 North Atlantic nitrogen budget, *Global Biogeochem. Cycles*, 20(3), n/a–n/a,  
 664 doi:10.1029/2005GB002456, 2006.
- 665 Fennel, K., Brady, D., DiToro, D., Fulweiler, R. W., Gardner, W. S., Giblin, A., McCarthy, M.  
 666 J., Rao, A., Seitzinger, S., Thouvenot-Korppoo, M. and Tobias, C.: Modeling denitrification in  
 667 aquatic sediments, *Biogeochemistry*, 93(1-2), 159–178, doi:10.1007/s10533-008-9270-z, 2008.
- 668 Fennel, K., Hu, J., Laurent, A., Marta-Almeida, M. and Hetland, R.: Sensitivity of hypoxia  
 669 predictions for the northern Gulf of Mexico to sediment oxygen consumption and model nesting,  
 670 *J. Geophys. Res. Ocean.*, 118(2), 990–1002, doi:10.1002/jgrc.20077, 2013.
- 671 Fogel, D. B.: An introduction to simulated evolutionary optimization., *IEEE Trans. neural*  
 672 *networks*, 5(1), 3–14, doi:10.1109/72.265956, 1994.
- 673 Friedrichs, M. A. M.: A data assimilative marine ecosystem model of the central equatorial  
 674 Pacific: Numerical twin experiments, *J. Mar. Res.*, 59(6), 859–894,  
 675 doi:10.1357/00222400160497544, 2001.
- 676 Friedrichs, M. A. M., Dusenberry, J. A., Anderson, L. A., Armstrong, R. A., Chai, F., Christian,  
 677 J. R., Doney, S. C., Dunne, J., Fujii, M., Hood, R., McGillicuddy, D. J., Moore, J. K., Schartau,  
 678 M., Spitz, Y. H. and Wiggert, J. D.: Assessment of skill and portability in regional marine

- 679 biogeochemical models: Role of multiple planktonic groups, *J. Geophys. Res.*, 112(C8), C08001,  
 680 doi:10.1029/2006JC003852, 2007.
- 681 Gardner, W. S., Briones, E. E., Kaegi, E. C. and Rowe, G. T.: Ammonium Excretion by Benthic  
 682 Invertebrates and Sediment-Water Nitrogen Flux in the Gulf of Mexico near the Mississippi  
 683 River Outflow, *Estuaries*, 16(4), 799, doi:10.2307/1352438, 1993.
- 684 Gypens, N., Lancelot, C. and Soetaert, K.: Simple parameterisations for describing N and P  
 685 diagenetic processes: Application in the North Sea, *Prog. Oceanogr.*, 76(1), 89–110,  
 686 doi:10.1016/j.pocean.2007.10.003, 2008.
- 687 Herman, P. M. J., Middelburg, J. J., Van de Koppel, J. and Hep, C. H. R.: Ecology of Estuarine  
 688 Macrobenthos, *Adv. Ecol. Res.*, 29, 195–240, 1999.
- 689 Hetland, R. D. and DiMarco, S. F.: How does the character of oxygen demand control the  
 690 structure of hypoxia on the Texas–Louisiana continental shelf?, *J. Mar. Syst.*, 70(1-2), 49–62,  
 691 doi:10.1016/j.jmarsys.2007.03.002, 2008.
- 692 Hibbert, D. B.: Genetic algorithms in chemistry, *Chemom. Intell. Lab. Syst.*, 19(3), 277–293,  
 693 doi:10.1016/0169-7439(93)80028-G, 1993.
- 694 Justić, D. and Wang, L.: Assessing temporal and spatial variability of hypoxia over the inner  
 695 Louisiana–upper Texas shelf: Application of an unstructured-grid three-dimensional coupled  
 696 hydrodynamic-water quality model, *Cont. Shelf Res.*, 72, 163–179,  
 697 doi:10.1016/j.csr.2013.08.006, 2014.
- 698 Justić, D., Rabalais, N. N. and Turner, R. E.: Effects of climate change on hypoxia in coastal  
 699 waters : a doubled CO<sub>2</sub> scenario for the northern Gulf of Mexico, , 41(5), 992–1003, 1996.
- 700 Kane, A., Moulin, C., Thiria, S., Bopp, L., Berrada, M., Tagliabue, A., Crépon, M., Aumont, O.  
 701 and Badran, F.: Improving the parameters of a global ocean biogeochemical model via  
 702 variational assimilation of in situ data at five time series stations, *J. Geophys. Res.*, 116(C6),  
 703 C06011, doi:10.1029/2009JC006005, 2011.
- 704 Kemp, W. M., Sampou, P., Cafrey, J., Mayer, M., Henriksen, K. and Boynton, W. R.:  
 705 Ammonium recycling versus denitrification Chesapeake Bay sediments, *Limnol. Oceanogr.*,  
 706 35(7), 1545–1563, doi:10.4319/lo.1990.35.7.1545, 1990.
- 707 Kolda, T. G., Lewis, R. M. and Torczon, V.: Optimization by direct search: New perspectives on  
 708 some classical and modern methods, *SIAM Rev.*, 45(3), 385–482, doi:Doi  
 709 10.1137/S003614450242889, 2003.
- 710 Kuhn, A. M., Fennel, K. and Mattern, J. P.: Model investigations of the North Atlantic spring  
 711 bloom initiation, *Prog. Oceanogr.*, doi:10.1016/j.pocean.2015.07.004, 2015.
- 712 Lehrter, J. C., Murrell, M. C. and Kurtz, J. C.: Interactions between freshwater input, light, and

- 713 phytoplankton dynamics on the Louisiana continental shelf, *Cont Shelf Res*, 29(15), 1861–1872,  
714 doi:10.1016/j.csr.2009.07.001, 2009.
- 715 Lehrter, J. C., Beddick, D., Devereux, R., Yates, D. and Murrell, M.: Sediment-water fluxes of  
716 dissolved inorganic carbon, O<sub>2</sub>, nutrients, and N<sub>2</sub> from the hypoxic region of the Louisiana  
717 continental shelf, *Biogeochemistry*, 109, 233–252, doi:10.1007/s10533-011-9623-x, 2012.
- 718 Li, Y.-H. and Gregory, S.: Diffusion of ions in the sea water and in deep-sea sediments,  
719 *Geochim. Cosmochim. Acta*, 38, 703–714, 1974.
- 720 Lin, X., McCarthy, M. J., Carini, S. A. and Gardner, W. S.: Net, actual, and potential sediment–  
721 water interface NH<sub>4</sub> fluxes in the northern Gulf of Mexico (NGOMEX): Evidence for NH<sub>4</sub>  
722 limitation of microbial dynamics, , 31, 120–128, doi:10.1016/j.csr.2010.11.012, 2011.
- 723 Lin, S. and Morse, J. W.: Sulfate reduction and iron sulfide mineral formation in Gulf of Mexico  
724 anoxic sediments, *Am. J. Sci.*, 291(1), 55–89, doi:10.2475/ajs.291.1.55, 1991.
- 725 Liu, K.-K., Atkinson, L., Quiñones, R. A. and Talaue-McManus, L.: Biogeochemistry of  
726 continental margins in a global context, in *Carbon and nutrient fluxes in continental margins*,  
727 edited by K.-K. Liu, L. Atkinson, R. A. Quiñones, and L. Talaue-McManus, Springer, Berlin.,  
728 2010.
- 729 McCarthy, M. J., Newell, S. E., Carini, S. a. and Gardner, W. S.: Denitrification Dominates  
730 Sediment Nitrogen Removal and Is Enhanced by Bottom-Water Hypoxia in the Northern Gulf of  
731 Mexico, *Estuaries and Coasts*, doi:10.1007/s12237-015-9964-0, 2015.
- 732 Middelburg, J. J. and Levin, L. a.: Coastal hypoxia and sediment biogeochemistry,  
733 *Biogeosciences*, 6(7), 1273–1293, doi:10.5194/bg-6-1273-2009, 2009.
- 734 Middelburg, J. J. and Soetaert, K.: The role of sediments in shelf ecosystem dynamics, in *The*  
735 *global coastal ocean. Multiscale interdisciplinary processes*, vol. 13, edited by A. R. Robinson  
736 and K. H. Brink, pp. 353–373, John Wiley & Sons, New York., 2005.
- 737 Middelburg, J. J., Soetaert, K., Herman, P. M. J. and Heip, C. H. R.: Denitrification in marine  
738 sediments : A model study, *Global Biogeochem. Cycles*, 10(4), 661–673,  
739 doi:10.1029/96GB02562, 1996.
- 740 Morse, J. W. and Berner, R. A.: What determines sedimentary C/S ratios?, *Geochim.*  
741 *Cosmochim. Acta*, 59(6), 1073–1077, doi:10.1016/0016-7037(95)00024-T, 1995.
- 742 Morse, J. W. and Eldridge, P. M.: A non-steady state diagenetic model for changes in sediment  
743 biogeochemistry in response to seasonally hypoxic/anoxic conditions in the “dead zone” of the  
744 Louisiana shelf, *Mar. Chem.*, 106(1-2), 239–255, doi:10.1016/j.marchem.2006.02.003, 2007.
- 745 Mulsow, S., Boudreau, B. P. and Smith, J. A.: Bioturbation and porosity gradients, *Limnol.*  
746 *Oceanogr.*, 43(1), 1–9, doi:10.4319/lo.1998.43.1.0001, 1998.

- 747 Murrell, M. C. and Lehrter, J. C.: Sediment and lower water column oxygen consumption in the  
 748 seasonally hypoxic region of the Louisiana continental shelf, *Estuaries and Coasts*, 34, 912–924,  
 749 doi: 10.1007/s12237-010-9351-9, 2011.
- 750 Neubacher, E. C., Parker, R. E. and Trimmer, M.: The potential effect of sustained hypoxia on  
 751 nitrogen cycling in sediment from the southern North Sea: a mesocosm experiment,  
 752 *Biogeochemistry*, 113(1-3), 69–84, doi:10.1007/s10533-012-9749-5, 2012.
- 753 Nunnally, C. C., Rowe, G. T., Thornton, D. C. O. and Quigg, A.: Sedimentary Oxygen  
 754 Consumption and Nutrient Regeneration in the Northern Gulf of Mexico Hypoxic Zone, *J. Coast.*  
 755 *Res.*, 63, 84–96, doi:10.2112/SI63-008.1, 2013.
- 756 Rabalais, N., Turner, R. E., Dortch, Q., Justić, D., Bierman, V. and Wiseman, W.: Nutrient-  
 757 enhanced productivity in the northern Gulf of Mexico: past, present and future, *Hydrobiologia*,  
 758 475–476(1), 39–63, doi:10.1023/A:1020388503274, 2002.
- 759 Rabouille, C., Mackenzie, F. T. and Ver, L. M.: Influence of the human perturbation on carbon,  
 760 nitrogen, and oxygen biogeochemical cycles in the global coastal ocean, *Geochim. Cosmochim.*  
 761 *Acta*, 65(21), 3615–3641, doi:10.1016/S0016-7037(01)00760-8, 2001.
- 762 Redalje, D. G., Lohrenz, S. E. and Fahnenstiel, G. L.: The Relationship between Primary  
 763 Production and the Vertical Export of Particulate Organic Matter in a River-Impacted Coastal  
 764 Ecosystem, *Estuaries*, 17(4), 829, doi:10.2307/1352751, 1994.
- 765 Redfield, A., Ketchum, B. and Richards, F.: The influence of organisms on the composition of  
 766 sea-water, in *The Sea*, Vol 2, vol. 2, edited by M. N. Hill, pp. 26–77, John Wiley & Sons, Inc.,  
 767 1963.
- 768 Robson, B., Hamilton, D., Webster, I. and Chan, T.: Ten steps applied to development and  
 769 evaluation of process-based biogeochemical models of estuaries, *Environ. Model. Softw.*, 23(4),  
 770 369–384, doi:10.1016/j.envsoft.2007.05.019, 2008.
- 771 Rowe, G. T. and Chapman, P.: Continental shelf hypoxia: some nagging questions, *Gulf Mex.*  
 772 *Sci.*, 2, 155–160, 2002.
- 773 Rowe, G. T., Cruz Kaegi, M. E., Morse, J. W., Boland, G. S. and Escobar Briones, E. G.:  
 774 Sediment community metabolism associated with continental shelf hypoxia, Northern Gulf of  
 775 Mexico, *Estuaries*, 25(6), 1097–1106, doi:10.1007/BF02692207, 2002.
- 776 Schartau, M. and Oschlies, A.: Simultaneous data-based optimization of a 1D-ecosystem model  
 777 at three locations in the North Atlantic: Part I—Method and parameter estimates, *J. Mar. Res.*,  
 778 61(6), 765–793, doi:10.1357/002224003322981147, 2003.
- 779 Soetaert, K. and Herman, P. M. J.: Nitrogen dynamics in the Westerschelde estuary (SW  
 780 Netherlands) estimated by means of the ecosystem model MOSES, *Hydrobiologia*, 311(1-3),

- 781 225–246, doi:10.1007/BF00008583, 1995.
- 782 Soetaert, K. and Petzoldt, T.: Inverse Modelling, Sensitivity and Monte Carlo Analysis in R  
783 Using Package FME, *J. Stat. Softw.*, 33(3), doi:10.18637/jss.v033.i03, 2010.
- 784 Soetaert, K., Herman, P. M. J. and Middelburg, J. J.: A model of early diagenetic processes from  
785 the shelf to abyssal depths, *Geochim. Cosmochim. Acta*, 60(6), 1019–1040, doi:10.1016/0016-  
786 7037(96)00013-0, 1996a.
- 787 Soetaert, K., Herman, P. M. J. and Middelburg, J. J.: Dynamic response of deep-sea sediments to  
788 seasonal variations: A model, *Limnol Ocean.*, 41(8), 1651–1668, 1996b.
- 789 Soetaert, K., Herman, P. M. J., Middelburg, J. J. and Heip, C.: Assessing organic matter  
790 mineralization, degradability and mixing rate in an ocean margin sediment (Northeast Atlantic)  
791 by diagenetic modeling, *J. Mar. Res.*, 56(2), 519–534, doi:10.1357/002224098321822401, 1998.
- 792 Soetaert, K., Middelburg, J. J., Herman, P. M. J. and Buis, K.: On the coupling of benthic and  
793 pelagic biogeochemical models, *Earth-Science Rev.*, 51(1-4), 173–201, doi:10.1016/S0012-  
794 8252(00)00004-0, 2000.
- 795 Ward, B. a., Friedrichs, M. a. M., Anderson, T. R. and Oschlies, A.: Parameter optimisation  
796 techniques and the problem of underdetermination in marine biogeochemical models, *J. Mar.*  
797 *Syst.*, 81(1-2), 34–43, doi:10.1016/j.jmarsys.2009.12.005, 2010.
- 798 Wilson, R. F., Fennel, K. and Paul Mattern, J.: Simulating sediment–water exchange of nutrients  
799 and oxygen: A comparative assessment of models against mesocosm observations, *Cont. Shelf*  
800 *Res.*, 63, 69–84, doi:10.1016/j.csr.2013.05.003, 2013.
- 801 Wood, C. C., Statham, P. J., Kelly-Gerreyn, B. a. and Martin, A. P.: Modelling macronutrients in  
802 shelf sea sediments: fitting model output to experimental data using a genetic algorithm, *J. Soils*  
803 *Sediments*, 14(1), 218–229, doi:10.1007/s11368-013-0793-0, 2013.
- 804

805 Table 1. Bottom water conditions at stations Z02 and Z03 in 2006. These data are used as forcing  
 806 conditions during the optimization of the diagenetic model. POM deposition flux ( $F_{\text{POM}}$ ) was not  
 807 measured;  $F_{\text{POM}}$  monthly climatologies were calculated for station Z02 and Z03 from a multiyear  
 808 simulation with a biogeochemical circulation model (see Section 2.3).

Station	Date	$F_{\text{POM}}$ mmol N m <sup>-2</sup> d <sup>-1</sup>	Temperature °C	NO <sub>3</sub> <sup>-</sup> mmol m <sup>-3</sup>	NH <sub>4</sub> <sup>+</sup> mmol m <sup>-3</sup>	O <sub>2</sub> mmol m <sup>-3</sup>
	April	3.53	21.6	7.16	0.58	60.2
Z02	June	2.19	24.0	8.61	7.93	0.0
	September	0.95	29.6	8.45	0.32	16.0
	April	1.36	21.7	1.50	0.47	67.9
Z03	June	1.20	25.7	1.90	2.40	137.9
	September	0.44	29.1	5.63	0.82	118.4

809

810 Table 2. Diagenetic model parameters. The 20 parameters that were optimized are indicated with  
 811 a + sign. The original values are from Soetaert et al. (1996a); an asterisk indicates values that are  
 812 identical in the optimized parameter set.

Symbol	Value		Parameter description	Units	Range
	optimized	original			
<b>H</b>	*	10	Active sediment depth	cm	–
<b>Φ<sub>0</sub></b>	*	0.8	Porosity at surface		–
<b>Φ<sub>∞</sub></b>	*	0.7	Porosity at depth H		–
<b>Φ<sub>coef</sub></b>	*	4.0	Porosity decay coefficient	cm <sup>-1</sup>	–
<b>w<sub>sed</sub></b>	0.416	0.022	(+) Burial velocity	cm y <sup>-1</sup>	0.05–1
<b>D<sub>NH4</sub></b>	*	0.847	Diffusion coefficient for ammonium at 0°C	cm <sup>2</sup> d <sup>-1</sup>	–
<b>D<sub>NO3</sub></b>	*	0.845	Diffusion coefficient for nitrate at 0°C	cm <sup>2</sup> d <sup>-1</sup>	–
<b>D<sub>O2</sub></b>	*	0.955	Diffusion coefficient for oxygen at 0°C	cm <sup>2</sup> d <sup>-1</sup>	–
<b>D<sub>ODU</sub></b>	*	0.842	Diffusion coefficient for ODU at 0°C	cm <sup>2</sup> d <sup>-1</sup>	–
<b>a<sub>NH4</sub></b>	*	0.0336	T-dependent coefficient for ammonium diffusion	cm <sup>2</sup> d <sup>-1</sup> (°C) <sup>-1</sup>	–
<b>a<sub>NO3</sub></b>	*	0.0303	T-dependent coefficient for nitrate diffusion	cm <sup>2</sup> d <sup>-1</sup> (°C) <sup>-1</sup>	–
<b>a<sub>O2</sub></b>	*	0.0386	T-dependent coefficient for oxygen diffusion	cm <sup>2</sup> d <sup>-1</sup> (°C) <sup>-1</sup>	–
<b>a<sub>ODU</sub></b>	*	0.0242	T-dependent coefficient for ODU diffusion	cm <sup>2</sup> d <sup>-1</sup> (°C) <sup>-1</sup>	–
<b>Z<sub>bio</sub></b>	1.0	5.0	(+) Depth of bioturbated layer	cm	1–7
<b>Dbio<sub>0</sub></b>	8.784	1.53	(+) Bioturbation "diffusivity"	cm <sup>2</sup> y <sup>-1</sup>	1–65
<b>Db<sub>coeff</sub></b>	*	1.0	Exponential decay below bioturbated layer	cm <sup>-1</sup>	–
<b>R<sub>1</sub><sup>T<sub>opt</sub></sup></b>	0.0213	0.02	(+) Remineralization at T <sub>opt</sub> for slow decaying OM1 pool	yr <sup>-1</sup>	10 <sup>-4</sup> –10 <sup>-1</sup>
<b>R<sub>2</sub><sup>T<sub>opt</sub></sup></b>	2.821	2.0	(+) Remineralization at T <sub>opt</sub> for fast decaying OM2 pool	yr <sup>-1</sup>	0.1–30
<b>PB</b>	0.00	0.05	(+) Part of ODUs permanently buried per day	d <sup>-1</sup>	0–0.95
<b>k<sub>O2</sub></b>	20.0	3.0	(+) Half-saturation, O <sub>2</sub> limitation on aerobic remineralization	μmolO <sub>2</sub> L <sup>-1</sup>	0.1–20
<b>kin<sub>odu</sub></b>	0.1	5.0	(+) Half-saturation, O <sub>2</sub> inhibition on anaerobic remin.	μmolO <sub>2</sub> L <sup>-1</sup>	0.1–20
<b>ox<sub>odu</sub></b>	11.45	20.0	(+) Maximum oxidation rate of ODUs	day <sup>-1</sup>	0.1–50
<b>k<sub>odu</sub></b>	20.0	1.0	(+) Half-saturation, O <sub>2</sub> in ODU oxidation	μmolO <sub>2</sub> L <sup>-1</sup>	0.1–20
<b>Nit</b>	50.0	20.0	(+) Maximum nitrification rate	day <sup>-1</sup>	0.05–50
<b>k<sub>nit</sub></b>	0.1	1.0	(+) Half-saturation, O <sub>2</sub> inhibition on nitrification	μmolO <sub>2</sub> L <sup>-1</sup>	0.1–10
<b>k<sub>dnt</sub></b>	1.0	30.0	(+) Half-saturation, nitrate limitation of denitrification	μmolNO <sub>3</sub> L <sup>-1</sup>	1–60
<b>kin<sub>dnt</sub></b>	30.0	10.0	(+) O <sub>2</sub> inhibition of denitrification	μmolO <sub>2</sub> L <sup>-1</sup>	1–30
<b>kin<sub>anox</sub></b>	0.1	5.0	(+) Half-saturation, nitrate inhibition of anaerobic remin.	μmolO <sub>2</sub> L <sup>-1</sup>	0.1–20
<b>θ<sub>r1</sub></b>	3.0	–	(+) Q <sub>10</sub> parameter for r <sub>1</sub>		2–3
<b>θ<sub>r2</sub></b>	3.0	–	(+) Q <sub>10</sub> parameter for r <sub>2</sub>		2–3
<b>θ<sub>bio</sub></b>	2.0	–	(+) Q <sub>10</sub> parameter for the bioturbation of solids		2–3
<b>T<sub>b</sub></b>	30.0	–	(+) Base temperature for Q <sub>10</sub> relationship	°C	20–30
<b>α<sub>0</sub></b>	0.0002	–	(+) Non-local mixing coefficient	yr <sup>-1</sup>	0–100

813

814 Table 3. Cost  $F(\mathbf{p})$ , calculated using Equation 3, for each variable type at station Z02 and Z03.  
 815 Simulations were run with the parameter set from Soetaert et al (1996a) (original) and with the  
 816 optimized parameter set (baseline). Additional optimizations were carried out for each station  
 817 independently (site-specific), for each station using sediment-water fluxes only (site-specific,  
 818 fluxes only), and including POM depositional flux in the optimization (site-specific, fluxes only,  
 819 +  $F_{POM}$ ).

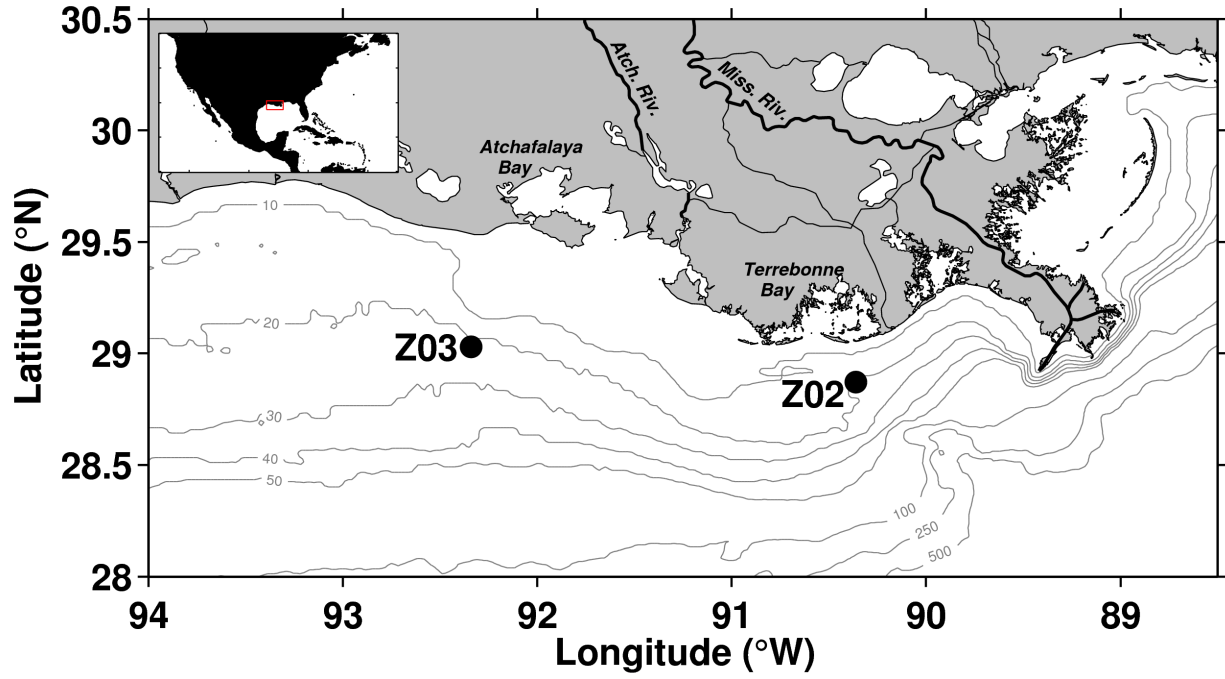
Optimization	Station	$F_{O_2}$	$F_{NH_4^+}$	$F_{NO_3^-}$	$NH_4^+$ profiles	Total
<i>Original</i>	Z02	0.1	366.2	107.8	1.5	475.6
	Z03	3.1	2788.3	1388.4	9.0	4188.8
	Total	3.2	3154.5	1496.2	10.5	4664.4
<i>Baseline</i>	Z02	0.2	8.6	52.6	1.5	62.9
	Z03	3.8	34.1	137.0	8.1	183.0
	Total	4.0	42.7	189.6	9.6	245.9
<i>Site-specific</i>	Z02	0.3	6.7	4.3	6.0	17.3
	Z03	3.9	25.7	134.0	8.9	172.5
	Total	4.2	32.4	138.3	14.9	189.8
<i>Site-specific, flux only</i>	Z02	0.4	5.0	3.8	-	9.3
	Z03	3.5	20.7	116.9	-	141.1
	Total	3.9	25.7	120.7	-	150.3
<i>Site-specific, flux only + <math>F_{POM}</math></i>	Z02	0.6	0.2	0.0	-	0.8
	Z03	5.4	2.9	68.5	-	76.8
	Total	6.0	3.1	68.5	-	77.6

820

821 Table 4. Meta-model coefficients for sediment O<sub>2</sub> consumption (F<sub>O<sub>2</sub></sub>), NH<sub>4</sub> flux (F<sub>NH<sub>4</sub><sup>+</sup></sub>) and NO<sub>3</sub><sup>-</sup>  
 822 flux (F<sub>NO<sub>3</sub><sup>-</sup></sub>). The form of the relationship is given in Eq. 4. For each flux, the average  
 823 contribution of each input variable is indicated as well as the dominant direction of its effect. A  
 824 positive effect promotes a weaker flux into the sediment or a larger flux to the water column  
 825 (depending on the direction of the flux) whereas a negative effect leads to a larger sink into the  
 826 sediment or a weaker flux to the water column. +/- indicates that the effect's direction varies as a  
 827 function of the variable. The contributions were calculated from standardized coefficients. Bold  
 828 values indicate variables contributing > 10% in average.

	Constant	F <sub>POM</sub> mmol N m <sup>-2</sup> d <sup>-1</sup>	Salinity	Temperature °C	NH <sub>4</sub> <sup>+</sup> mmol m <sup>-3</sup>	NO <sub>3</sub> <sup>-</sup> mmol m <sup>-3</sup>	O <sub>2</sub> mmol m <sup>-3</sup>	
Data range		0.1 – 62.1	0 – 36.4	15.1 – 36.0	0.1 – 24.7	0 – 161.2	0 – 475.1	
F <sub>O<sub>2</sub></sub>	x <sub>i</sub>	22.1151	-1.3381	0.8138	-7.1247	0.4592	-0.8055	-0.0721
	x <sub>i</sub> <sup>2</sup>		0.0286	0.0868	0.3668	-0.2074	0.0229	-0.0001
	x <sub>i</sub> <sup>3</sup>		-0.0001	-0.0023	-0.0069	0.0112	-0.0001	0.0000
	Contribution (%)		5.0	<b>20.3</b>	<b>55.4</b>	1.9	<b>10.4</b>	6.9
	Effect direction		-	+	-	+/-	+/-	+/-
F <sub>NH<sub>4</sub></sub>	x <sub>i</sub>	-10.8192	0.0740	-0.0833	2.0967	-0.2221	0.0836	-0.0283
	x <sub>i</sub> <sup>2</sup>		0.0023	-0.0064	-0.0996	0.0500	-0.0024	0.0002
	x <sub>i</sub> <sup>3</sup>		-0.0001	0.0002	0.0016	-0.0023	0.0000	-0.0000
	Contribution (%)		1.5	<b>11.4</b>	<b>59.1</b>	3.3	5.4	<b>19.3</b>
	Effect direction		+/-	-	+	+/-	+/-	-
F <sub>NO<sub>3</sub></sub>	x <sub>i</sub>	3.6115	-0.0071	0.0463	-0.5613	0.1142	-0.0134	0.0144
	x <sub>i</sub> <sup>2</sup>		-0.0014	-0.0035	0.0238	-0.0209	0.0001	-0.0001
	x <sub>i</sub> <sup>3</sup>		0.0000	0.0001	-0.0003	0.0008	-0.0000	0.0000
	Contribution (%)		0.8	<b>12.8</b>	<b>54.1</b>	5.2	2.6	<b>24.5</b>
	Effect direction		-	+/-	-	+/-	-	+

829



830

Figure 1. Map of the Louisiana Shelf showing the location of sample collection sites Z02 and Z03.

831

832

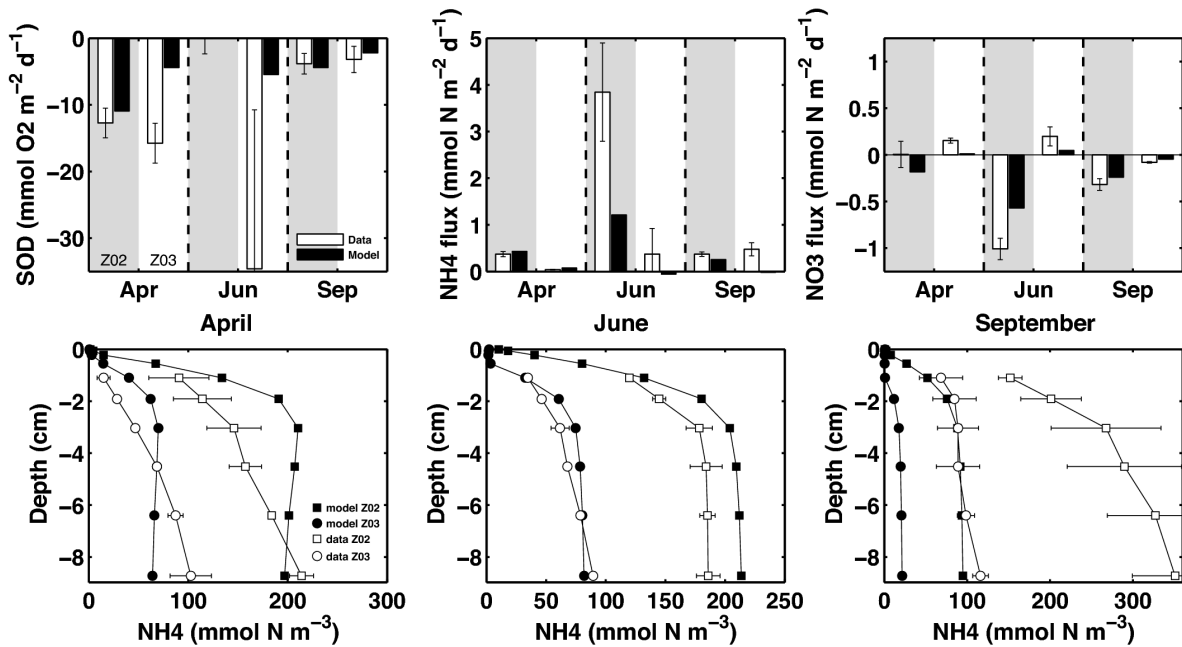
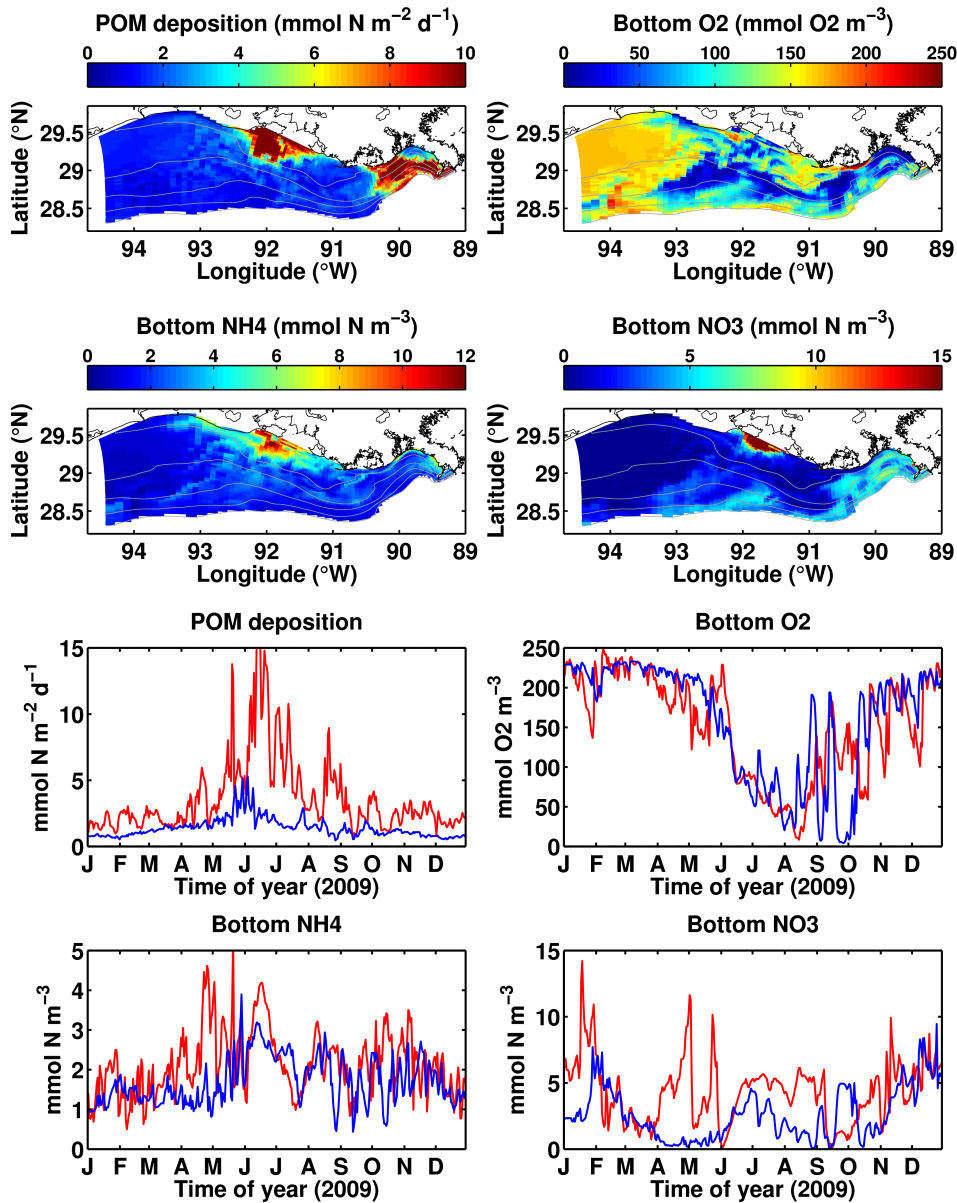


Figure 2. Model-data comparison of sediment water fluxes (top row) and  $\text{NH}_4^+$  profiles (bottom row) for sites Z02 and Z03. Simulations use the optimized parameter set (baseline).

834



835

836 Figure 3. Spatial (top) and temporal (bottom) POM depositional flux and bottom water O<sub>2</sub>, NH<sub>4</sub><sup>+</sup>

837 and NO<sub>3</sub><sup>-</sup> concentrations in the biogeochemical circulation model. The upper panels represent a

838 snapshot of bottom water conditions on August 15<sup>th</sup>, 2009 and the lower panels time series at

839 stations Z02 and Z03. This dataset is used to force the diagenetic model in the meta-modeling

840 procedure (Section 2.2), to compute spatial fluxes with the meta-model (Figure 8) and to  
841 compare the meta-model and H&D parameterizations (Figure 12).

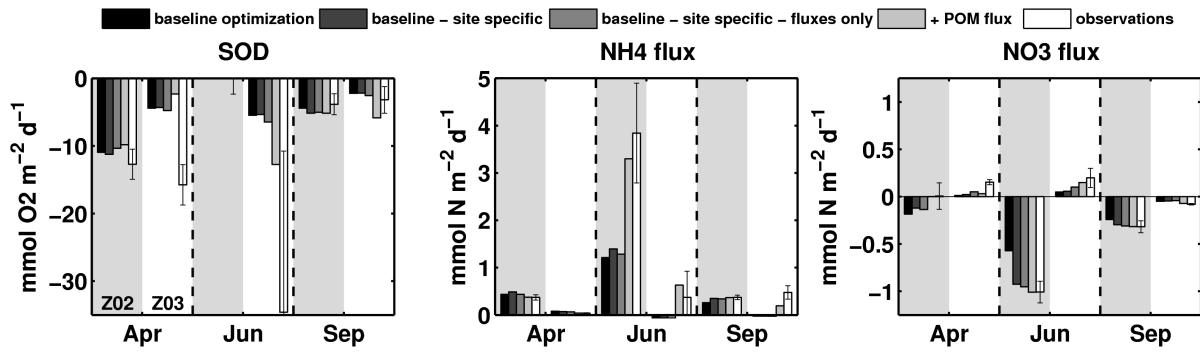


Figure 4. Model-data comparison of sediment water fluxes at stations Z02 and Z03 for several different optimization schemes (baseline includes all constraints).

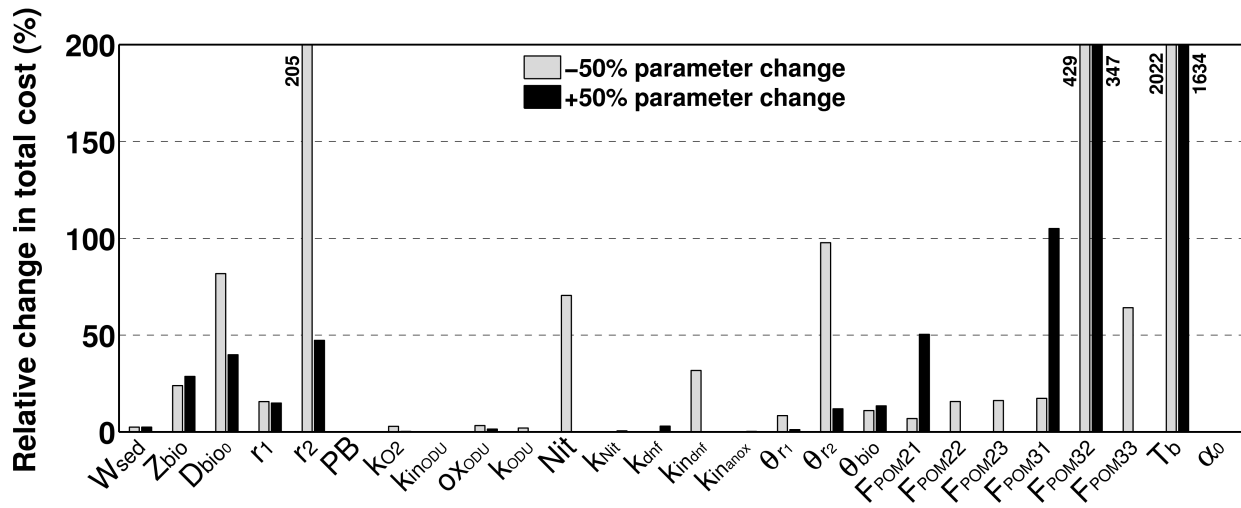


Figure 5. Sensitivity of model results to parameter variation.

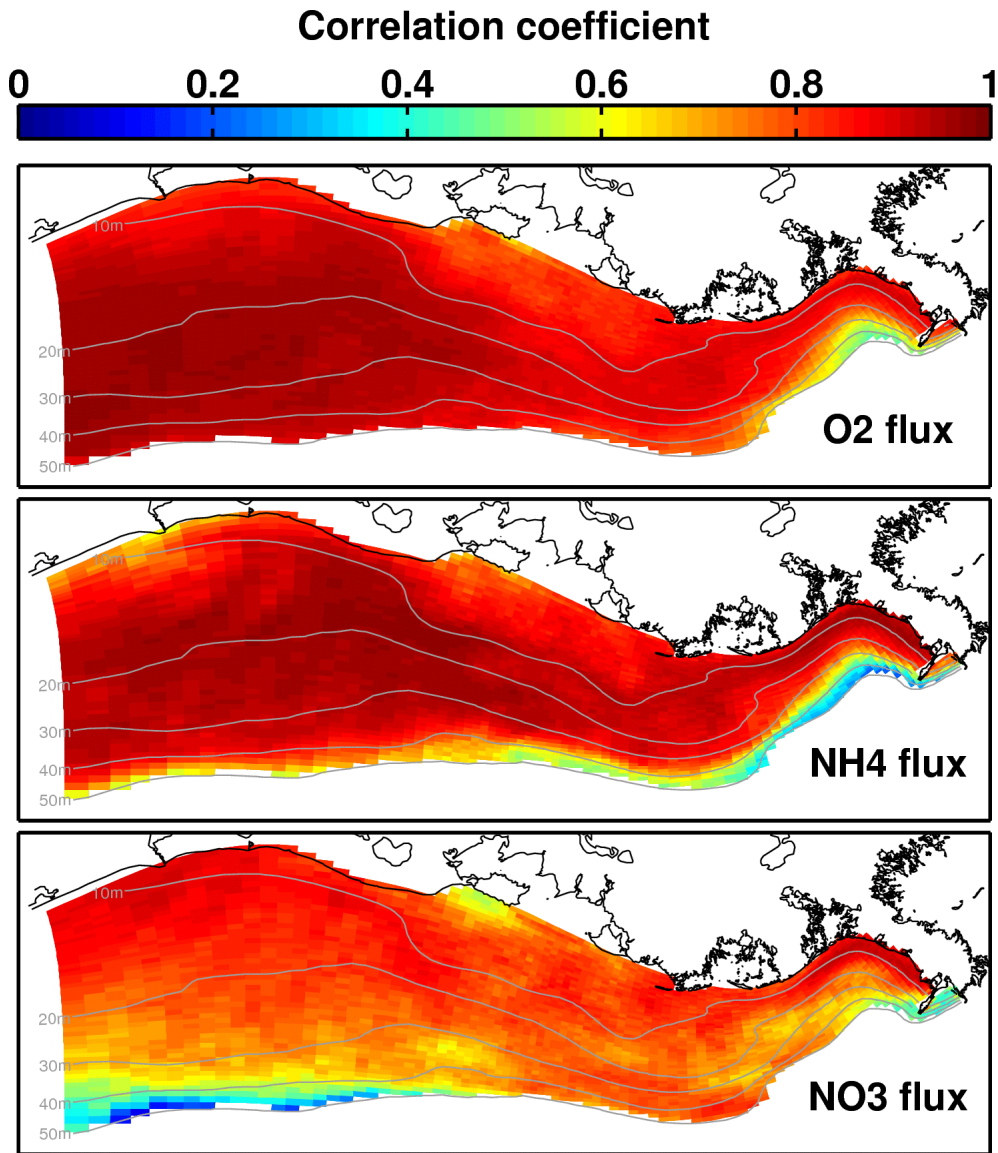


Figure 6. Correlation coefficients between time-dependent diagenetic model simulations and the parameterized fluxes for each location on the Louisiana Shelf.

845

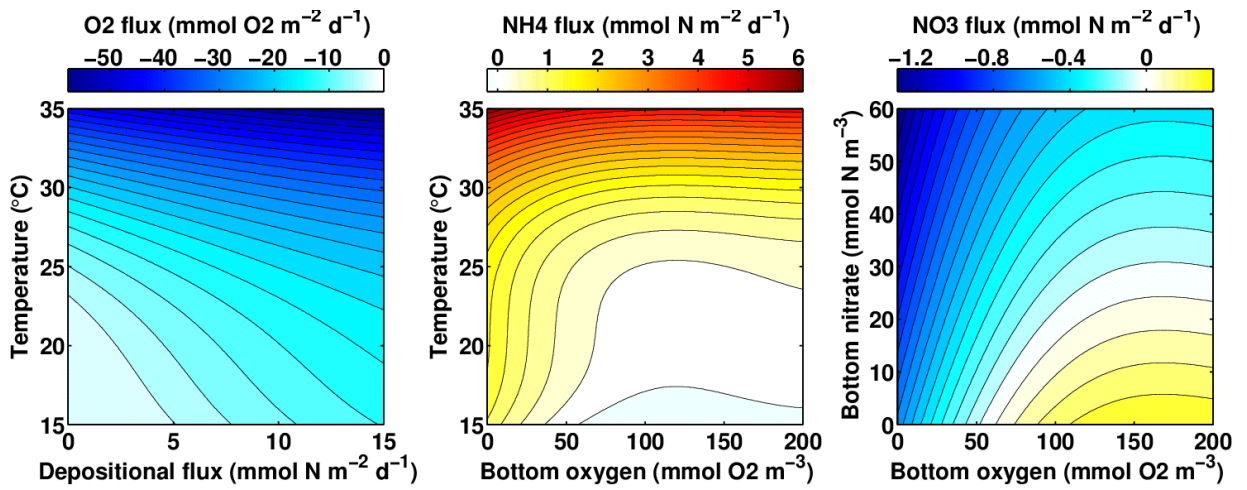


Figure 7. Influence of selected contributors to  $O_2$ ,  $NH_4^+$  and  $NO_3^-$  fluxes. Negative fluxes (blue shades) are into the sediment and positive fluxes (orange shades) are out of the sediment.

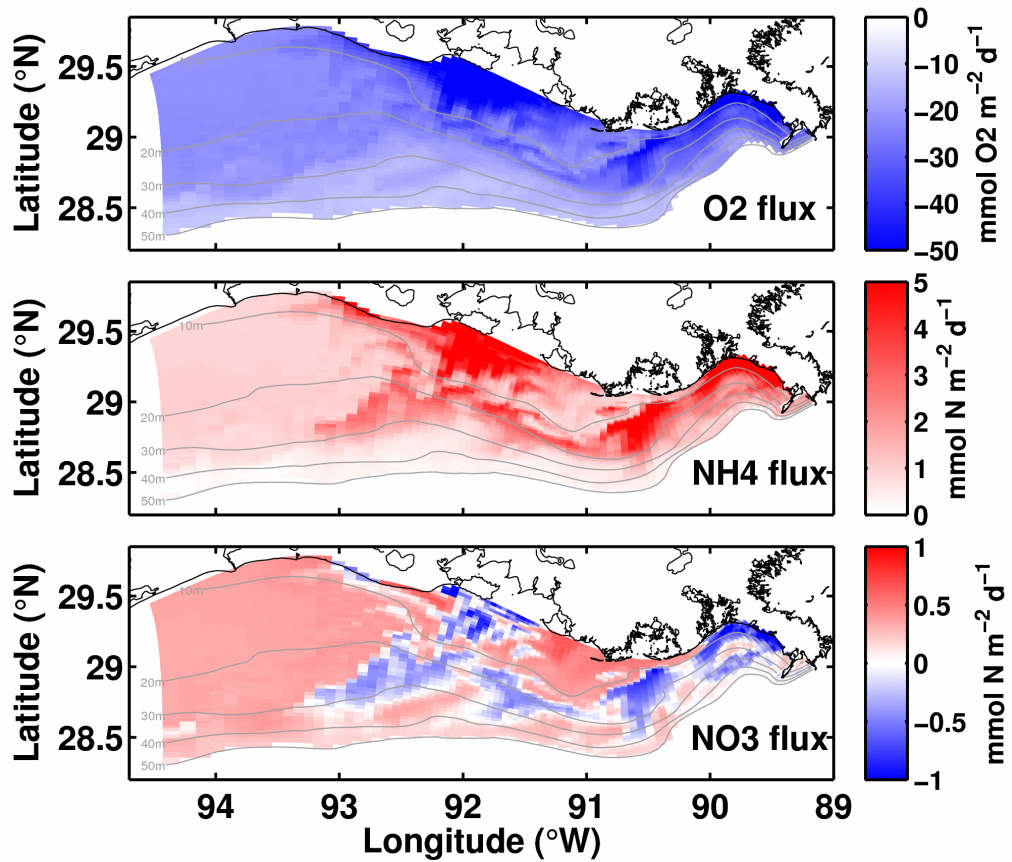
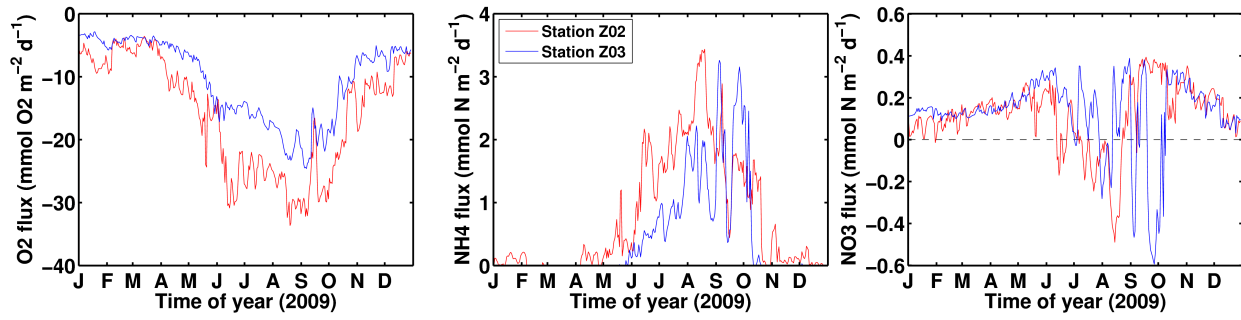


Figure 8. Spatial distribution of parameterized  $O_2$ ,  $NH_4^+$  and  $NO_3^-$  fluxes on August 15<sup>th</sup>, 2009. Negative fluxes (blue) are into the sediment.

847



848

849 Figure 9. Temporal variability of parameterized O<sub>2</sub>, NH<sub>4</sub><sup>+</sup> and NO<sub>3</sub><sup>-</sup> fluxes at station Z02 and Z03  
850 in 2009. Negative fluxes are into the sediment.

851

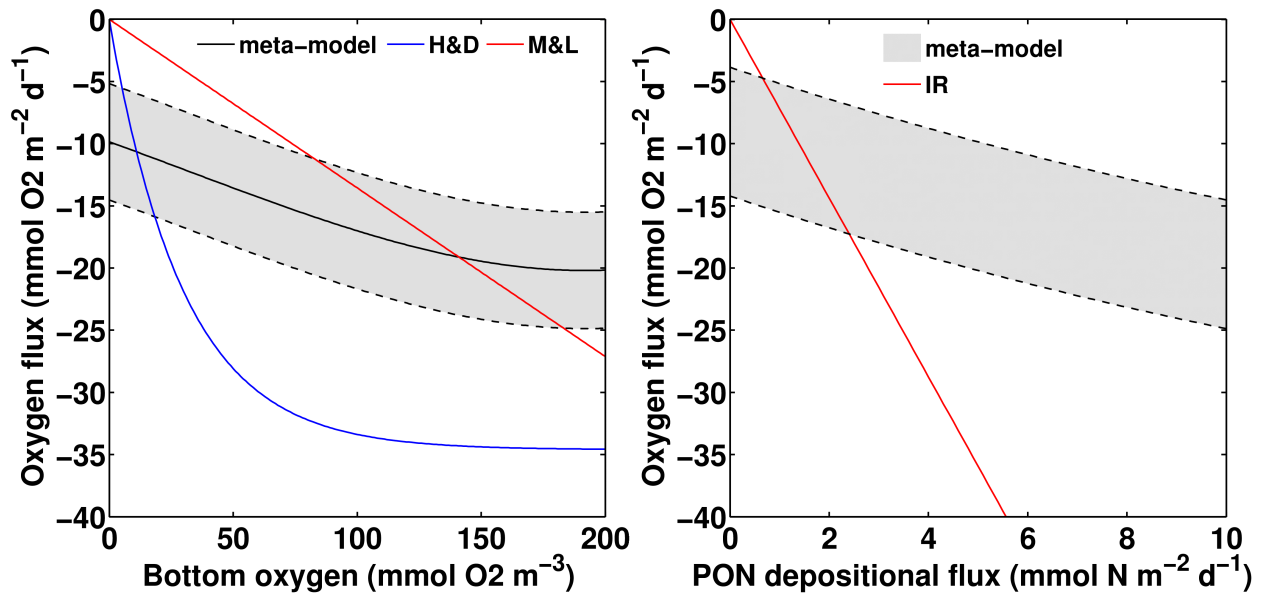


Figure 10. O<sub>2</sub> flux in the meta-model compared to that from the IR, H&D and M&L parameterizations as a function of bottom O<sub>2</sub> concentration (left) and of POM depositional flux (right). The grey area and the black line on the left panel corresponds to the variation in O<sub>2</sub> flux when  $1 < F_{\text{POM}} < 10 \text{ mmol N m}^{-2} \text{ d}^{-1}$  and  $F_{\text{POM}} = 5 \text{ mmol N m}^{-2} \text{ d}^{-1}$ , respectively. The grey area on the right panel corresponds to the variation in O<sub>2</sub> flux when bottom O<sub>2</sub> concentration range from 0 to 200 mmol O<sub>2</sub> m<sup>-3</sup>. The comparison between H&D, M&L and SOC observations can be found in Fennel et al (2013) and Yu et al (2015).

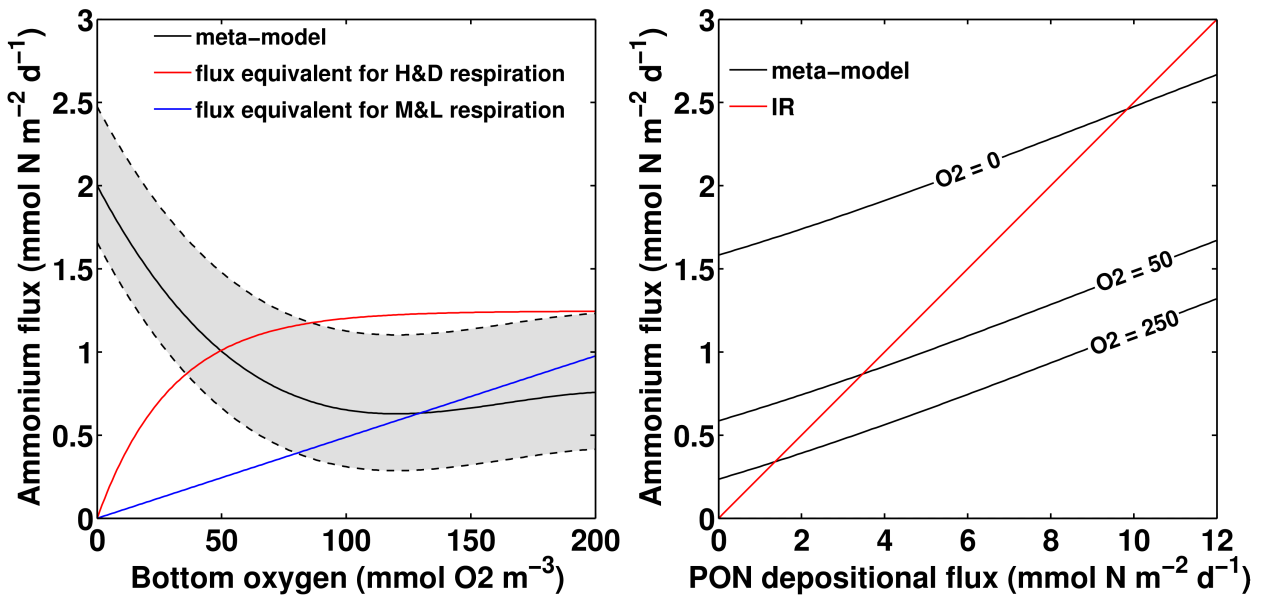


Figure 11.  $\text{NH}_4^+$  flux in the meta-model compared with that from the IR, H&D and M&L parameterizations.  $\text{NH}_4^+$  flux is represented as a function of (left) bottom  $\text{O}_2$  concentration and (right) PON depositional flux. The grey area and the black line on the left panel correspond to the variation in  $\text{O}_2$  flux when  $1 < F_{\text{POM}} < 10 \text{ mmol N m}^{-2} \text{ d}^{-1}$  and  $F_{\text{POM}} = 5 \text{ mmol N m}^{-2} \text{ d}^{-1}$ , respectively. The black lines on the right indicate the  $\text{O}_2$  flux at bottom  $\text{O}_2$  concentrations of 0, 50 and 250  $\text{mmol O}_2 \text{ m}^{-3}$ .

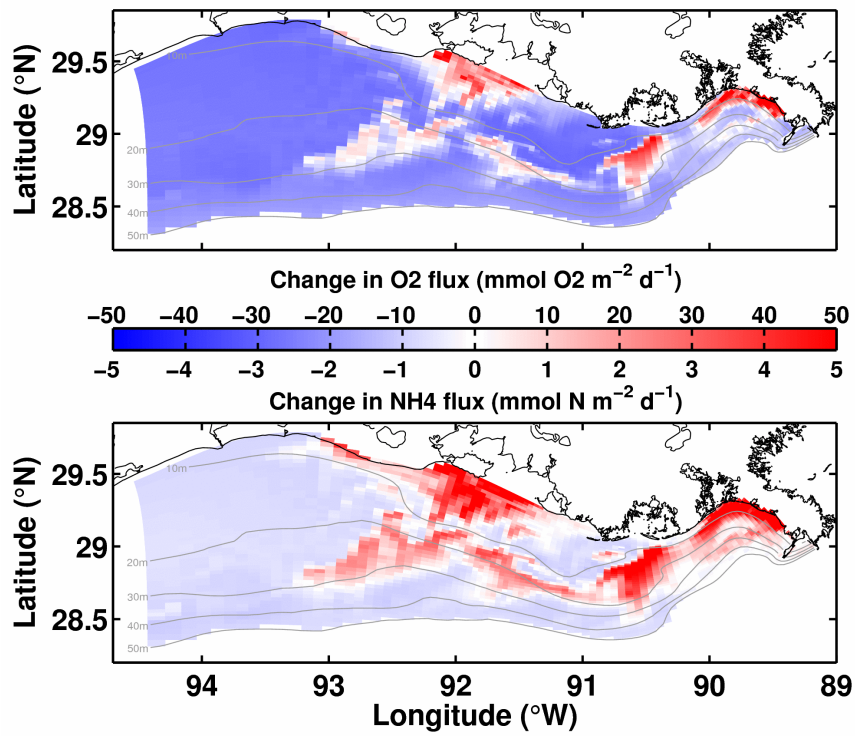


Figure 12. Difference between parameterized oxygen (top panel) and ammonium (bottom panel) fluxes and fluxes simulated with the H&D parameterization in August 15<sup>th</sup>, 2009.